Is Value Functions Estimation with Classification Plug-and-play for Offline Reinforcement Learning?

Anonymous authors
Paper under double-blind review

Abstract

In deep Reinforcement Learning (RL), value functions are typically approximated using deep neural networks and trained via mean squared error regression objectives to fit the true value functions. Recent research has proposed an alternative approach, utilizing the cross-entropy classification objective, which has demonstrated improved performance and scalability of RL algorithms. However, existing study have not extensively benchmarked the effects of this replacement across various domains, as the primary objective was to demonstrate the efficacy of the concept across a broad spectrum of tasks, without delving into in-depth analysis. Our work seeks to empirically investigate the impact of such a replacement in an offline RL setup and analyze the effects of different aspects on performance. Through large-scale experiments conducted across a diverse range of tasks using different algorithms, we aim to gain deeper insights into the implications of this approach. Our results reveal that incorporating this change can lead to superior performance over state-of-the-art solutions for some algorithms in certain tasks, while maintaining comparable performance levels in other tasks, however for other algorithms this modification might lead to the dramatic performance drop. This findings are crucial for further application of classification approach in research and practical tasks.

1 Introduction

In the realm of deep Reinforcement Learning (RL), the conventional approach to approximating value functions has long relied on employing the Bellman optimality operator alongside mean squared error (MSE) regression objectives, owing to the continuous nature of the task at hand. However, insights from other domains of machine learning have illuminated the potential benefits of employing classification objectives even in scenarios where regression seems as a natural choice (Rothe et al., 2018; Rogez et al., 2019). This shift has been attributed to various hypotheses, including the stability of gradients (Imani et al., 2024), improved feature representation (Zhang et al., 2023), and implicit biases (Stewart et al., 2023).

While the use of regression loss has yielded remarkable results in value-based RL (Silver et al., 2017), it also presents certain challenges and limitations (Kumar et al., 2020a; 2021; Agarwal et al., 2021; Lyle et al., 2022). Notably, recent research Farebrother et al. (2024) has demonstrated that replacing regression with classification for training value functions offers several advantages, including enhanced scalability, feature representation, performance, and robustness to noisy targets and non-stationarity. While this study broadly explores the effects of this replacement, it does not delve deeply into the ease of implementation or the impact of newly introduced hyperparameters.

Offline RL (Levine et al., 2020) represents a rapidly developing RL subfield, wherein the objective is to train an agent using a pre-collected dataset without direct interaction with the environment. In recent years, numerous algorithms have been developed to address this setup (Kumar et al., 2020b; Fujimoto & Gu, 2021; Kostrikov et al., 2021; An et al., 2021; Chen et al., 2021; Akimov et al., 2022; Yang et al., 2022; Ghasemipour et al., 2022; Nikulin et al., 2023; Tarasov et al., 2024a). The majority of these algorithms fall under the category of off-policy value-based approaches, owing to their alignment with the problem setup's requirements.

Given the prevalence of off-policy value-based approaches in offline RL, it becomes imperative to delve deeper into the potential impact of employing classification for value function training within this domain. While Farebrother et al. (2024) offer some experimental insights into offline RL tasks, we contend that there remain significant gaps to be addressed. Therefore, our study seeks to contribute to this area by conducting a thorough investigation into the utilization of classification objectives for value function training in offline RL scenarios.

This study aims to address the following questions through large-scale experiments conducted on a large range of tasks from the standard D4RL benchmark (Fu et al., 2020):

- Is classification a "plug-and-play replacement" for offline RL algorithms, and how does it impact performance?
- Does the use of classification objectives facilitate a more robust hyperparameter search?
- What is the impact of the hyperparameters introduced with classification?
- Does classification enable more efficient scaling of dense neural networks compared to regression?

2 Preliminaries

2.1 Offline Reinforcement Learning

The RL problem is conventionally framed as a Markov Decision Process characterized by a tuple S, A, P, R, γ, where: $S \subset \mathbb{R}^n$ denotes the state space, $A \subset \mathbb{R}^m$ represents the action space, $P : S \times A \to S$ is the transition function, $R : S \times A \to \mathbb{R}$ is the reward function, and $\gamma \in (0, 1)$ is the discount factor. The objective RL of is to determine a policy (agent) $\pi : S \to A$ that maximizes the expected sum of discounted rewards: $\sum_{t=0}^{\infty} \gamma^t R(s_t, a_t)$. This entails the policy learning process, where the agent interacts with its environment by observing environmental states, taking actions in response, and receiving corresponding rewards.

Offline RL presents a departure from the traditional RL setup in that the agent relies solely on a pre-collected dataset D collected by external agents. This paradigm introduces novel challenges, such as the estimation of value functions for out-of-distribution state-action pairs, thus giving rise to an entire subfield dedicated to addressing these challenges.

2.2 Q-function objective and classification

The Q-function stands as a pivotal concept in value-based RL, representing the expected return of a policy starting from state s_t and taking action a_t: $Q(s_t, a_t) = \mathbb{E}_\pi[\sum_{k=0}^{\infty} \gamma^k R(s_{t+k}, a_{t+k})|s_t, a_t]$. Typically, value functions are trained using the Bellman optimality operator:

$$(\hat{\mathcal{T}}Q)(s, a, \hat{\theta}) = R(s, a) + \gamma \max_{a'} Q(s', a', \hat{\theta})$$

Here, s' denotes the state observed after executing action a at state s, and $\hat{\theta}$ (also known as target network) represents a copy with delayed updates of the parameter θ which parametrize the value function. During each training step, parameters θ are adjusted using temporal difference (TD) error with mean squared error (MSE):

$$\mathrm{TD}_{\mathrm{MSE}}(\theta) = \mathbb{E}_D((\hat{\mathcal{T}}Q)(s_t, a_t, \hat{\theta}) - Q(s_t, a_t, \theta))^2$$

We adopt the framework proposed by Farebrother et al. (2024) for replacing MSE with cross-entropy loss. The approach involves parameterizing the Q-function as a distribution over returns, segmented into m bins with widths ζ, where the first bin corresponds to the predefined v_{min} value, and the last to v_{max}. The scalar value of the Q-function is then computed as:

$$Q(s, a, \theta) = \mathbb{E}[Z(s, a, \theta)], \quad Z(s, a, \theta) = \sum_{i=1}^{m} p_i(s, a, \theta)\delta_i,$$

where p_i represents the probability of the i-th bin, and δ_i denotes the corresponding bin value. This formulation allows us to express the TD error using cross-entropy and utilize it for updating the value function parameters:

$$\mathrm{TD}_{\mathrm{CE}}(\theta) = \mathbb{E}_D \sum_{i=1}^{m} p_i^{\mathcal{T}}(s, a, \hat{\theta}) \log p_i(s, a, \theta)$$

Farebrother et al. (2024) demonstrated that the HL-Gauss method (Imani & White, 2018) is particularly effective for mapping continuous values into bins within this framework. HL-Gauss employs a normal distribution analog for mapping values into neighboring bins, with a hyperparameter σ determining the distribution's breadth. The authors recommend tuning the ratio σ/ζ as a more interpretable hyperparameter, with a default value of 0.75 chosen based on statistical considerations and it has shown good empirical result.

3 Methodology

Our methodology is straightforward: we select several offline RL algorithms and adapt them for cross-entropy loss, as outlined in Section 2.2. By default, we determine the values of v_{min} and v_{max} by computing all possible discounted returns within a given dataset and identifying the minimum and maximum values, which aligns naturally with the offline RL setup. Herein, we provide brief descriptions of the algorithms employed in our study.

Revisited BRAC (ReBRAC). ReBRAC (Tarasov et al., 2024a) stands as a minimalist, state-of-the-art ensemble-free algorithm for both offline and offline-to-online RL. It employs MSE to penalize deviations from actions present in the dataset. Built upon TD3+BC (Fujimoto & Gu, 2021), ReBRAC incorporates several modifications that significantly enhance its performance. The Q-loss function takes the form:

$$\mathbb{E}_{(s,a,s',\hat{a'})\sim D, a'\sim\pi(s')}(Q(s,a,\theta) - [R(s,a) + \gamma(Q(s',a',\hat{\theta}) - \beta(a' - \hat{a'})^2)])^2$$

where β denotes a penalty weight. Although only the target network part differs, the bin mapping is conducted in the same manner, with the penalty subtracted beforehand. We select ReBRAC as an exemplary algorithm with policy regularization due to its high performance, simplicity, and its encounter with the Q-function divergence problem while solving certain D4RL AntMaze tasks.

Implicit Q-Learning (IQL). IQL (Kostrikov et al., 2021) represents another competitive offline and offline-to-online RL algorithm. Its key advantage lies in its exclusion of out-of-distribution examples during training, a departure from most other offline RL approaches. This is achieved through the training of the V-function: $V(s_t) = \mathbb{E}_\pi[\sum_{k=0}^{\infty} \gamma^k R(s_{t+k}, a_{t+k})|s_t]$. The Q-function loss takes the form:

$$\mathbb{E}_{(s,a,s')\sim D}(Q(s,a,\theta) - [R(s,a) + \gamma V_\phi(s')])^2$$

Once again, the target component allows for classification without additional manipulations. Regularization is achieved through a specially designed V-function loss, without explicit penalties for the policy or value functions. We opt for IQL as it the best example of algorithms within this family.

Large-Batch SAC (LB-SAC). LB-SAC (Nikulin et al., 2022) is an instance of the ensemble-based SAC-N algorithm (An et al., 2021), utilizing large-batch optimization to reduce ensemble size. SAC-N comprises N Q-functions, each with the following loss:

$$\mathbb{E}_{(s,a,s')\sim D, a'\sim\pi(s')}(Q(s,a,\theta_i) - [R(s,a) + \gamma \min_{j=1..N} Q(s',a',\hat{\theta}_j)])^2$$

No additional adjustments are necessary to replace MSE with cross-entropy. The rationale behind this objective lies in the assumption that if Q-values follow a normal distribution $\mathcal{N}(\mu, \sigma)$ then:

$$\min_{j=1..N} Q(s,a,\hat{\theta}_j) \approx \mu(s,a) - \Phi^{-1}\left(\frac{N - \frac{\pi}{8}}{N - \frac{\pi}{4} + 1}\right)\sigma(s,a)$$

Ensemble-based approaches are known for their efficacy across many offline RL tasks. According to the above statement, SAC-N can be also considered as an example of offline RL algorithm with Q-function regularization. We opt for LB-SAC instead of the original SAC-N due to computational constraints.

4 Experimental Results

4.1 Experimental setup

We conducted our experiments using three sets of tasks from the D4RL benchmark (Fu et al., 2020): Gym-MuJoCo, AntMaze, and Adroit. We utilized all datasets within each set.

For ReBRAC in subsection 4.2, we employed the best hyperparameters as outlined in Tarasov et al. (2024a). When exploring parameter search in, we utilized the same hyperparameter grids for ReBRAC and IQL and used a custom grid for LB-SAC due to computational constraints. For a comprehensive overview of the experimental details and hyperparameters, refer to Appendix A and Appendix B.

The evaluation protocol is taken from Tarasov et al. (2024a), where hyperparameters search is done using four random seeds and separate set of seeds is used for the evaluation with the exception that we utilized four random seeds for the final evaluation instead of ten, due to computational constraints. Note, that because of the chosen evaluation protocol tuned hyperparameters might perform worse than non-tuned which characterizes the sensitivity to the random initialization.

4.2 Is classification plug-and-play?

Our initial goal was to substitute MSE with cross-entropy without modifying any other aspects of the algorithms. We fixed the number of bins m to 101, representing a reasonable number of classes. We set $\sigma/\zeta = 0.75$ by default as was proposed by Farebrother et al. (2024). Results for this modification are presented in the **CE** columns of Table 1 for Gym-MuJoCo, Table 2 for AntMaze, and Table 3 for Adroit. We also provide rliable (Agarwal et al., 2021) metrics which support all of the further claims in a more readable way in Appendix H. It is worth noting that, for ReBRAC in the AntMaze tasks here and further, we used large-batch optimization, similar to that used in Gym-MuJoCo, which was previously hindered by Q-function divergence.

The original ReBRAC algorithm exhibited minimal performance variation with the introduction of cross-entropy in Gym-MuJoCo tasks, except for the random dataset where a notable performance drop was observed. However, on average, the score remained relatively stable. In the case of AntMaze, where ReBRAC faced Q-function divergence issues, the introduction of classification mitigated this problem, resulting in notable improvement in average performance. However, in Adroit, where ReBRAC struggled with overfitting due to small dataset sizes, classification did not alleviate this issue and led to decreased performance across most scenarios.

In contrast, both IQL and LB-SAC experienced a significant performance drop in Gym-MuJoCo tasks. IQL's performance in AntMaze dramatically decreased, rendering the algorithm unable to solve medium and large tasks with this modification. Meanwhile, LB-SAC's performance did not change significantly for AntMaze but improved for the umaze task. Notably, in the Adroit task, IQL's performance was significantly boosted in the pen environment, with relatively minor changes observed in other scenarios. However, LB-SAC's performance dropped across most tasks.

Our primary hypothesis for explaining the successful application of classification with ReBRAC and its failure with IQL and LB-SAC is that ReBRAC heavily relies on policy regularization. Consequently, plugging classification into Q networks does not strongly affect its offline RL component compared to the impact observed in IQL or LB-SAC.

4.3 Algorithms hyperparameters search with classification

The subsequent step in our investigation involved determining whether better performance could be achieved by tuning the hyperparameters of the original algorithms. The evaluation of the best hyperparameter sets can be found under the **CE+AT** columns in Table 1, Table 2, and Table 3 (see also Appendix H).

[1]These notations are reused further.

Table 1: Average normalized score over the final evaluation and ten (four for LB-SAC) unseen random seeds on Gym-MuJoCo tasks. "hc" stands for "halfcheetah", "hp" stands for "hopper", "wl" stands for "walker2d", "r" stands for "random", "m" stands for "medium", "e" stands for "expert", "me" stands for "medium-expert", "mr" stands for "medium-replay", "fr" stands for "full-replay". **MSE** denotes original algorithm implementation, **CE** denotes the replacement of MSE with cross-entropy, **CE+AT** denotes cross-entropy with tuned algorithm parameters, **CE+CT** denotes cross-entropy with tuned classification parameters[1]. ReBRAC original scores are taken from Tarasov et al. (2024a).

	ReBRAC				IQL				LB-SAC			
Task	**MSE**	**CE**	**CE+AT**	**CE+CT**	**MSE**	**CE**	**CE+AT**	**CE+CT**	**MSE**	**CE**	**CE+AT**	**CE+CT**
hc-r	29.5 ± 1.5	13.4 ± 0.8	13.4 ± 0.8	13.0 ± 0.8	18.9 ± 1.0	1.9 ± 0.0	6.7 ± 0.9	3.9 ± 2.5	28.2 ± 1.4	10.0 ± 0.3	11.6 ± 0.2	11.1 ± 0.7
hc-m	65.6 ± 1.0	59.5 ± 0.7	63.8 ± 1.4	58.2 ± 11.2	49.5 ± 1.1	42.5 ± 0.3	42.6 ± 0.4	43.8 ± 0.3	64.5 ± 1.3	56.7 ± 2.1	63.6 ± 9.7	55.5 ± 2.7
hc-e	105.9 ± 1.7	103.2 ± 5.5	104.2 ± 2.5	103.7 ± 4.2	95.8 ± 2.2	92.9 ± 0.2	92.9 ± 0.4	93.5 ± 0.2	103.0 ± 1.5	103.9 ± 1.0	105.0 ± 1.3	104.5 ± 2.2
hc-me	101.1 ± 5.2	103.5 ± 4.3	103.2 ± 5.5	101.6 ± 6.4	92.3 ± 2.4	86.5 ± 4.0	83.3 ± 3.4	89.0 ± 3.8	104.5 ± 2.4	105.4 ± 2.0	105.2 ± 0.0	107.2 ± 1.3
hc-mr	51.0 ± 0.8	50.7 ± 0.7	53.1 ± 1.3	50.4 ± 2.3	45.2 ± 0.5	38.1 ± 1.8	39.9 ± 1.1	40.6 ± 1.8	52.8 ± 0.7	55.4 ± 0.9	54.4 ± 1.6	58.1 ± 1.3
hc-fr	82.1 ± 1.1	83.2 ± 1.5	82.4 ± 1.9	83.4 ± 0.9	75.5 ± 0.5	62.6 ± 1.1	64.5 ± 1.5	74.1 ± 0.6	79.0 ± 2.0	80.7 ± 0.3	81.3 ± 1.0	82.3 ± 1.1
hp-r	8.1 ± 2.4	8.1 ± 0.9	8.9 ± 2.1	9.1 ± 1.4	6.0 ± 2.8	14.2 ± 2.8	13.7 ± 3.3	13.8 ± 7.5	14.5 ± 11.5	8.2 ± 2.2	9.6 ± 0.4	10.9 ± 2.3
hp-m	102.0 ± 1.0	98.9 ± 9.4	101.7 ± 1.6	98.1 ± 7.5	54.8 ± 4.4	54.1 ± 2.0	52.9 ± 3.6	53.5 ± 1.8	90.0 ± 27.5	7.9 ± 0.8	10.5 ± 6.2	7.8 ± 1.0
hp-e	100.1 ± 8.3	107.9 ± 4.9	107.9 ± 4.9	110.8 ± 0.5	109.4 ± 1.8	110.5 ± 0.5	110.6 ± 0.3	110.2 ± 1.0	1.3 ± 0.0	21.6 ± 39.7	65.9 ± 51.9	12.3 ± 13.1
hp-me	107.0 ± 6.4	111.6 ± 0.5	111.2 ± 0.3	111.6 ± 0.5	88.5 ± 16.5	64.0 ± 10.2	69.3 ± 23.9	102.0 ± 8.6	111.3 ± 0.3	14.9 ± 7.0	12.5 ± 7.2	54.7 ± 37.6
hp-mr	98.1 ± 5.3	98.7 ± 3.0	94.1 ± 12.5	98.7 ± 3.0	95.9 ± 6.4	71.5 ± 10.1	27.2 ± 4.5	67.2 ± 8.8	63.0 ± 48.1	66.9 ± 42.8	100.6 ± 5.5	87.4 ± 29.6
hp-fr	107.1 ± 0.4	108.2 ± 0.3	108.3 ± 0.2	108.3 ± 0.5	107.2 ± 0.6	41.9 ± 4.8	53.9 ± 9.5	103.9 ± 0.6	107.0 ± 0.7	65.6 ± 50.2	109.9 ± 0.4	109.1 ± 1.8
wl-r	18.4 ± 4.5	8.8 ± 4.4	12.1 ± 9.1	7.2 ± 5.1	6.4 ± 6.3	3.9 ± 2.1	9.3 ± 7.6	6.3 ± 8.1	21.7 ± 0.0	20.1 ± 2.9	21.8 ± 0.0	21.5 ± 0.2
wl-m	82.5 ± 3.6	85.1 ± 2.7	85.1 ± 2.7	85.7 ± 1.0	83.2 ± 1.2	79.9 ± 1.3	81.3 ± 1.7	80.9 ± 1.5	89.3 ± 5.3	89.6 ± 10.7	93.7 ± 7.3	98.0 ± 1.3
wl-e	112.3 ± 0.2	112.7 ± 0.1	112.7 ± 0.1	112.7 ± 0.1	113.8 ± 0.2	108.5 ± 0.2	108.5 ± 0.2	109.5 ± 0.2	114.2 ± 0.4	59.8 ± 45.0	107.6 ± 1.2	112.5 ± 0.2
wl-me	111.6 ± 0.3	111.7 ± 0.1	111.9 ± 0.2	112.0 ± 0.3	112.3 ± 0.6	92.2 ± 6.5	108.6 ± 1.0	109.4 ± 0.1	110.6 ± 0.4	73.1 ± 18.1	94.0 ± 33.2	109.6 ± 8.8
wl-mr	77.3 ± 7.9	85.2 ± 6.7	84.4 ± 5.9	84.0 ± 5.0	82.0 ± 7.9	59.1 ± 8.8	67.2 ± 5.1	82.6 ± 3.8	92.6 ± 2.7	90.9 ± 5.3	95.3 ± 6.0	99.8 ± 1.9
wl-fr	102.2 ± 1.7	101.8 ± 5.6	108.7 ± 5.0	102.4 ± 2.9	97.7 ± 1.4	85.3 ± 3.3	83.9 ± 1.9	93.6 ± 1.0	102.1 ± 1.0	110.4 ± 1.9	109.4 ± 1.3	110.5 ± 2.4
Avg	81.2	80.6	81.5	80.6	74.1	61.6	62.0	70.9	74.9	57.8	69.5	69.6

Table 2: Average normalized score over the final evaluation and ten (four for LB-SAC) unseen random seeds on AntMaze tasks. "um" stands for "umaze", "med" stands for "medium", "lrg" stands for "large", "p" stands for "play", "d" stands for "diverse". ReBRAC original scores are taken from Tarasov et al. (2024a).

	ReBRAC				IQL				LB-SAC			
Task	**MSE**	**CE**	**CE+AT**	**CE+CT**	**MSE**	**CE**	**CE+AT**	**CE+CT**	**MSE**	**CE**	**CE+AT**	**CE+CT**
um	97.8 ± 1.0	98.0 ± 2.1	98.0 ± 1.6	98.8 ± 1.1	79.1 ± 6.8	50.0 ± 4.6	49.6 ± 8.1	53.0 ± 6.2	18.25 ± 35.8	41.0 ± 33.2	36.0 ± 33.4	57.5 ± 12.7
um-d	88.3 ± 13.0	93.0 ± 4.5	91.5 ± 8.0	94.5 ± 4.1	72.5 ± 4.5	48.7 ± 6.9	47.4 ± 5.3	48.8 ± 5.3	0.0 ± 0.0	0.0 ± 0.0	0.2 ± 0.5	0.0 ± 0.0
med-p	84.0 ± 4.2	88.0 ± 6.3	90.5 ± 3.8	88.1 ± 5.1	73.8 ± 5.4	0.2 ± 0.4	0.1 ± 0.3	0.4 ± 0.6	0.0 ± 0.0	0.0 ± 0.0	0.0 ± 0.0	0.0 ± 0.0
med-d	76.3 ± 13.5	84.8 ± 9.3	76.6 ± 14.8	90.0 ± 4.8	74.8 ± 3.8	0.4 ± 0.9	0.3 ± 0.6	0.3 ± 0.4	0.0 ± 0.0	0.0 ± 0.0	0.0 ± 0.0	0.0 ± 0.0
lrg-p	60.4 ± 26.1	85.9 ± 6.3	87.0 ± 4.3	87.8 ± 3.4	41.3 ± 7.0	0.0 ± 0.0	0.0 ± 0.0	0.0 ± 0.0	0.0 ± 0.0	0.0 ± 0.0	0.0 ± 0.0	0.0 ± 0.0
lrg-d	54.4 ± 25.1	87.1 ± 4.1	86.6 ± 4.6	81.9 ± 8.2	23.7 ± 5.6	0.0 ± 0.0	0.0 ± 0.0	0.0 ± 0.0	0.0 ± 0.0	0.0 ± 0.0	0.0 ± 0.0	0.0 ± 0.0
Avg	76.8	89.4	88.3	90.1	60.8	16.5	16.2	17.0	3.0	6.8	6.0	9.5

In Gym-MuJoCo tasks, these hyperparameter adjustments yielded slight improvements in ReBRAC's average performance, although random datasets remained problematic. Similarly, in Adroit tasks, performance saw some improvement but still fell short of the original algorithm's performance. Notably, for AntMaze tasks, the hyperparameter adjustments did not improve performance in this domain when compared to just plugging cross-entropy.

For IQL and LB-SAC, tuning the algorithms' hyperparameters with a cross-entropy objective helped alleviate underperformance in Gym-MuJoCo tasks, although random datasets remained a common issue. However, this approach did not yield significant improvements for AntMaze tasks, and only marginally improved average performance in Adroit.

Following the methodology outlined by Kurenkov & Kolesnikov (2022), we investigated whether algorithms utilizing classification offered superior hyperparameter search under uniform policy selection on D4RL tasks, using Expected Online Performance (EOP). The results are presented in Table 4 under the **CE+AT** rows. It is evident that for ReBRAC, classification facilitated much better hyperparameter search in the AntMaze domain, marginally improved search for Gym-MuJoCo, and showed slight degradation for Adroit tasks. IQL benefited only in the Adroit domain, while LB-SAC showed a slight improvement in AntMaze tasks.

Table 3: Average normalized score over the final evaluation and ten (four for LB-SAC) unseen random seeds on Adroit tasks. "ham" stands for "hammer", "rel" stands for "relocate", "h" stands for "human", "c" stands for "cloned", "e" stands for "expert". ReBRAC original scores are taken from Tarasov et al. (2024a).

	ReBRAC				IQL				LB-SAC			
Task	**MSE**	**CE**	**CE+AT**	**CE+CT**	**MSE**	**CE**	**CE+AT**	**CE+CT**	**MSE**	**CE**	**CE+AT**	**CE+CT**
pen-h	103.5 ± 14.1	102.3 ± 10.2	95.8 ± 15.5	97.5 ± 13.3	21.1 ± 16.8	108.2 ± 8.4	107.2 ± 13.0	93.6 ± 8.7	4.5 ± 2.6	7.1 ± 5.6	20.1 ± 19.6	5.8 ± 8.8
pen-c	91.8 ± 21.7	90.3 ± 14.2	94.0 ± 18.3	100.6 ± 16.2	13.2 ± 21.6	12.5 ± 14.7	99.9 ± 21.7	11.1 ± 15.0	26.1 ± 5.3	20.0 ± 4.5	20.8 ± 5.0	22.0 ± 8.0
pen-e	154.1 ± 5.4	155.0 ± 5.8	152.9 ± 4.4	155.9 ± 4.8	60.2 ± 37.7	134.9 ± 7.0	141.1 ± 8.5	141.3 ± 4.3	130.5 ± 16.8	38.0 ± 13.2	62.0 ± 9.3	43.6 ± 29.8
door-h	0.0 ± 0.0	0.0 ± 0.0	0.0 ± 0.0	0.0 ± 0.1	5.9 ± 2.5	4.3 ± 1.0	4.6 ± 2.9	3.4 ± 2.1	-0.2 ± 0.1	-0.2 ± 0.1	-0.2 ± 0.1	-0.2 ± 0.1
door-c	1.1 ± 2.6	0.0 ± 0.0	0.2 ± 0.4	0.0 ± 0.0	0.2 ± 0.3	0.3 ± 0.3	2.4 ± 1.1	1.2 ± 0.7	0.0 ± 0.0	0.2 ± 0.5	0.5 ± 1.0	0.0 ± 0.0
door-e	104.6 ± 2.4	105.7 ± 1.5	103.4 ± 4.2	105.0 ± 2.4	105.4 ± 2.0	106.1 ± 0.5	103.0 ± 3.0	105.7 ± 1.6	95.0 ± 8.6	70.6 ± 33.8	76.5 ± 5.5	68.7 ± 19.4
ham-h	0.2 ± 0.2	0.1 ± 0.1	0.4 ± 0.3	0.1 ± 0.1	1.7 ± 0.8	1.5 ± 0.7	2.1 ± 1.9	2.4 ± 1.6	0.1 ± 0.0	0.0 ± 0.0	0.1 ± 0.0	0.1 ± 0.0
ham-c	6.7 ± 3.7	9.7 ± 10.4	3.9 ± 4.9	6.1 ± 8.8	0.2 ± 0.0	1.0 ± 0.7	1.3 ± 0.6	2.6 ± 4.4	20.2 ± 16.8	13.6 ± 15.4	0.0 ± 0.0	19.9 ± 21.7
ham-e	133.8 ± 0.7	122.9 ± 19.7	120.1 ± 24.9	134.2 ± 1.0	129.5 ± 0.2	129.5 ± 0.1	129.5 ± 0.1	130.5 ± 0.2	76.6 ± 59.5	91.1 ± 10.5	96.0 ± 9.9	89.2 ± 11.2
rel-h	0.0 ± 0.0	0.0 ± 0.0	0.0 ± 0.0	0.0 ± 0.0	0.1 ± 0.1	0.1 ± 0.0	0.1 ± 0.1	0.1 ± 0.0	0.0 ± 0.0	-0.1 ± 0.0	0.0 ± 0.0	-0.1 ± 0.0
rel-c	0.9 ± 1.6	0.4 ± 0.5	0.3 ± 0.3	0.2 ± 0.2	0.1 ± 0.1	0.1 ± 0.1	0.1 ± 0.1	0.1 ± 0.0	0.0 ± 0.0	-0.1 ± 0.0	-0.1 ± 0.0	-0.1 ± 0.0
rel-e	106.6 ± 3.2	107.8 ± 3.3	107.2 ± 2.8	108.4 ± 2.5	108.2 ± 0.9	105.7 ± 1.8	109.4 ± 0.7	106.5 ± 1.8	26.7 ± 18.8	5.3 ± 3.5	5.1 ± 3.5	2.5 ± 4.3
Avg w/o e	25.5	25.3	24.3	25.5	5.3	16.0	27.2	14.3	6.3	5.0	5.1	5.9
Avg	58.6	57.8	56.5	59.0	37.1	50.3	58.3	42.5	31.6	20.4	23.4	20.9

4.4 What is the impact of classification parameters?

In Farebrother et al. (2024), the authors conducted a limited study on the influence of specific classification hyperparameters, only examining if $\sigma/\zeta = 0.75$ was suitable across varying numbers of bins m, using online RL tasks. Drawing inspiration from their work, we selected a set of m values: $21, 51, 101, 201, 401$, and a set of σ/ζ values: $0.55, 0.65, 0.75, 0.85$. Subsequently, we conducted experiments using all possible pairs of these parameters, while maintaining the parameters of the original algorithms.

Evaluation results, presented in Table 1, Table 2, and Table 3 under the **CE+CT** columns (see also Appendix H), showcased notable differences in the impact of tuning classification parameters across algorithms. Specifically, ReBRAC exhibited improved performance when classification hyperparameters were fine-tuned, surpassing the original version's efficacy and achieving new state-of-the-art performance on AntMaze. In contrast, IQL and LB-SAC did not consistently benefit from classification parameter tuning compared to algorithm-specific adjustments.

EOP for this hyperparameter search is also provided in Table 4 under the **+CE+CT** rows. It's evident that when having good hyperparameters for original algorithm tuning classification parameters yields greater benefits than tuning algorithm-specific hyperparameters, as expected, with the only exception of IQL on Adroit tasks. Additionally, this search converges quickly, with training approximately three different policies often sufficing to achieve near-optimal performance, a highly advantageous property for real-world application of offline RL.

We present algorithms' performance heatmaps for the parameter grid averaged over domains in Figure 1, with detailed scores per dataset available in Appendix I. Additionally, in Appendix E, we provide further insights by fixing one parameter and averaging over the second. Our analysis indicates that setting $m = 101$ and $\sigma/\zeta = 0.75$ may serve as a reasonable starting point and produce results better than the average. Notably, a higher number of classes often yields improved performance, suggesting a preference for larger m values. Regarding σ/ζ, our findings suggest that 0.75 remains a favorable choice, especially when faced with limited tuning resources. However, the optimal selection of classification parameters heavily depends on the specific algorithm, environment, and dataset characteristics.

Farebrother et al. (2024) did not investigate the impact of the v_{min} and v_{max} choices, nor did they propose a method for selecting these when the reward function is unknown. In our previous experiments, we computed these values by taking the minimum and maximum return across all possible sub-trajectories in the dataset. However, this approach may not be optimal because offline RL algorithms often introduce pessimism into the Q function. Additionally, setting these limits based on extreme values may cause the values on the edges of the support to differ from other values from the model's perspective, potentially impacting the final results.

[2] 9 policies for LB-SAC+CE+CT.

Table 4: Expected Online Performance (Kurenkov & Kolesnikov, 2022) under uniform policy selection aggregated over D4RL domains across four training seeds. This demonstrates the sensitivity to the choice of hyperparameters given a certain budget for online evaluation. **+CE+AT** denotes cross-entropy with tuned algorithm parameters, **+CE+CT** denotes cross-entropy with tuned classification parameters, **+CE+MT** denotes cross-entropy with mixed parameters tuning.

Domain	Algorithm	1 policy	2 policies	3 policies	5 policies	10 policies [2]	15 policies	18 policies	20 policies
Gym-MuJoCo	**ReBRAC**	62.0 ± 17.1	70.6 ± 9.9	73.3 ± 5.5	74.8 ± 2.1	75.6 ± 0.8	75.8 ± 0.6	75.9 ± 0.6	76.0 ± 0.5
	ReBRAC+CE+AT	64.1 ± 15.4	71.7 ± 8.7	74.0 ± 4.8	75.4 ± 1.9	76.2 ± 1.1	76.6 ± 1.0	76.7 ± 0.9	76.8 ± 0.8
	ReBRAC+CE+CT	78.4 ± 1.4	79.2 ± 1.2	79.7 ± 1.0	80.1 ± 0.7	80.5 ± 0.5	80.6 ± 0.4	80.7 ± 0.4	80.7 ± 0.3
	ReBRAC+CE+MT	62.0 ± 15.5	70.1 ± 10.5	73.3 ± 6.6	75.3 ± 2.9	76.4 ± 0.9	76.6 ± 0.5	76.7 ± 0.3	-
	IQL	62.3 ± 9.8	67.6 ± 6.0	69.5 ± 3.8	70.9 ± 1.9	71.6 ± 0.7	71.8 ± 0.4	71.9 ± 0.3	71.9 ± 0.3
	IQL+CE+AT	55.7 ± 4.2	58.1 ± 3.6	59.3 ± 2.8	60.5 ± 1.8	61.4 ± 0.9	61.7 ± 0.7	61.8 ± 0.6	61.8 ± 0.6
	IQL+CE+CT	58.4 ± 7.2	62.5 ± 5.6	64.4 ± 4.3	66.1 ± 2.6	67.2 ± 1.3	67.6 ± 1.0	67.8 ± 0.9	67.9 ± 0.9
	IQL+CE+MT	65.2 ± 3.6	67.2 ± 2.7	68.1 ± 2.0	68.9 ± 1.2	69.5 ± 0.6	69.7 ± 0.4	69.7 ± 0.3	-
	LB-SAC	52.5 ± 13.8	59.5 ± 8.3	62.0 ± 5.5	64.1 ± 3.8	-	-	-	-
	LB-SAC+CE+AT	48.9 ± 11.3	54.4 ± 7.0	56.4 ± 5.2	58.3 ± 4.1	-	-	-	-
	LB-SAC+CE+CT	63.4 ± 3.7	65.4 ± 2.4	66.2 ± 1.7	66.9 ± 1.0	67.3 ± 0.6	-	-	-
	LB-SAC+CE+MT	44.4 ± 11.1	50.5 ± 7.9	53.0 ± 5.4	55.0 ± 2.9	56.3 ± 1.5	56.8 ± 1.2	57.0 ± 1.0	-
AntMaze	**ReBRAC**	67.9 ± 10.0	73.6 ± 7.4	76.1 ± 5.5	78.3 ± 3.4	79.9 ± 1.7	80.4 ± 1.1	-	-
	ReBRAC+CE+AT	84.8 ± 4.9	87.5 ± 3.5	88.7 ± 2.5	89.7 ± 1.5	90.4 ± 0.8	90.7 ± 0.5	-	-
	ReBRAC+CE+CT	83.8 ± 10.3	88.3 ± 4.7	89.4 ± 2.2	90.0 ± 0.9	90.4 ± 0.6	90.6 ± 0.4	90.7 ± 0.4	90.7 ± 0.3
	ReBRAC+CE+MT	63.5 ± 33.0	79.8 ± 22.3	85.8 ± 13.7	89.2 ± 5.2	90.8 ± 1.4	91.2 ± 0.9	91.3 ± 0.7	-
	IQL	21.1 ± 5.4	24.1 ± 4.7	25.7 ± 4.2	27.5 ± 3.6	29.5 ± 2.7	30.4 ± 2.0	30.7 ± 1.7	30.9 ± 1.5
	IQL+CE+AT	15.6 ± 0.9	16.1 ± 0.8	16.4 ± 0.7	16.7 ± 0.7	17.0 ± 0.6	17.2 ± 0.5	17.3 ± 0.4	17.3 ± 0.4
	IQL+CE+CT	16.2 ± 0.7	16.6 ± 0.7	16.8 ± 0.7	17.1 ± 0.7	17.5 ± 0.6	17.7 ± 0.6	17.8 ± 0.5	17.8 ± 0.5
	IQL+CE+MT	23.3 ± 9.3	28.1 ± 9.9	31.2 ± 9.6	35.1 ± 8.3	39.2 ± 5.1	40.6 ± 3.0	41.0 ± 2.3	-
	LB-SAC	1.0 ± 1.4	1.6 ± 1.6	2.1 ± 1.6	2.8 ± 1.4	-	-	-	-
	LB-SAC+CE+AT	3.2 ± 3.9	5.1 ± 3.9	6.3 ± 3.4	7.6 ± 2.2	-	-	-	-
	LB-SAC+CE+CT	7.9 ± 1.5	8.7 ± 1.1	9.1 ± 0.9	9.4 ± 0.5	9.6 ± 0.3	-	-	-
	LB-SAC+CE+MT	2.8 ± 3.7	4.6 ± 4.0	6.0 ± 3.8	7.6 ± 3.1	9.2 ± 1.7	9.7 ± 1.0	9.8 ± 0.8	-
Adroit	**ReBRAC**	44.1 ± 18.4	53.2 ± 10.9	56.1 ± 6.1	57.8 ± 2.3	58.6 ± 0.9	58.9 ± 0.7	59.0 ± 0.7	59.1 ± 0.6
	ReBRAC+CE+AT	43.9 ± 17.1	52.7 ± 10.3	55.6 ± 6.0	57.5 ± 2.5	58.5 ± 0.9	58.7 ± 0.6	58.8 ± 0.6	58.9 ± 0.5
	ReBRAC+CE+CT	56.9 ± 1.7	57.9 ± 1.3	58.4 ± 1.0	58.8 ± 0.7	59.2 ± 0.4	59.3 ± 0.3	59.4 ± 0.3	59.4 ± 0.2
	ReBRAC+CE+MT	40.8 ± 17.0	49.8 ± 12.0	53.5 ± 8.1	56.3 ± 4.1	57.8 ± 1.4	58.0 ± 0.6	58.1 ± 0.4	-
	IQL	33.9 ± 2.3	35.2 ± 1.7	35.8 ± 1.5	36.4 ± 1.2	37.1 ± 0.9	37.4 ± 0.6	37.5 ± 0.6	37.5 ± 0.5
	IQL+CE+AT	53.0 ± 3.5	55.0 ± 3.1	56.1 ± 2.7	57.2 ± 1.9	58.1 ± 0.8	58.3 ± 0.4	58.4 ± 0.3	58.4 ± 0.3
	IQL+CE+CT	49.6 ± 1.3	50.4 ± 0.9	50.7 ± 0.7	51.0 ± 0.6	51.3 ± 0.4	51.4 ± 0.4	51.5 ± 0.3	51.5 ± 0.3
	IQL+CE+MT	54.2 ± 3.1	55.9 ± 2.3	56.7 ± 1.7	57.4 ± 1.0	57.8 ± 0.3	57.8 ± 0.1	57.8 ± 0.1	-
	LB-SAC	15.7 ± 14.1	23.4 ± 12.8	27.7 ± 10.5	31.7 ± 6.6	-	-	-	-
	LB-SAC+CE+AT	12.7 ± 8.0	17.1 ± 5.9	19.1 ± 4.3	20.6 ± 2.3	-	-	-	-
	LB-SAC+CE+CT	22.0 ± 2.7	23.4 ± 2.6	24.2 ± 2.7	25.2 ± 2.6	26.4 ± 2.2	-	-	-
	LB-SAC+CE+MT	12.5 ± 8.8	17.3 ± 6.5	19.4 ± 4.6	21.1 ± 2.6	22.3 ± 1.5	22.8 ± 1.2	23.0 ± 1.1	-

To evaluate the effect of these parameters, we computed the support size as $v_{max} - v_{min}$ from the dataset and multiplied this size by a parameter v_{expand}. We then extended the support in two ways: Subtracting $v_{expand}(v_{max} - v_{min})$ from v_{min} (referred to as *min*), and simultaneously subtracting from v_{min} and adding to v_{max} the term $v_{expand}(v_{max} - v_{min})/2$ (referred to as *both*)[3]. The experimental results, shown in Figure 5, demonstrate that our initial choice of support parameters was sub-optimal and increasing the support range may strongly benefit. Surprisingly, in some cases, reducing the support was beneficial. The *both* strategy generally yielded better performance.

Our observations support the assumption about efficiency of cross-entropy for offline RL algorithms with policy regularization compared to other types. Notably, ReBRAC exhibited less sensitivity to the classification parameters.

4.5 Do MLPs scale better with classification?

In Farebrother et al. (2024), authors emphasized the enhanced scalability of models when regression is replaced with classification, particularly when using Transformers or ResNets. In this subsection, we delve into whether similar scalability benefits apply to Multilayer Perceptrons (MLPs), which are commonly utilized

[3]The division by 2 ensures equal bin sizes across the two variants.

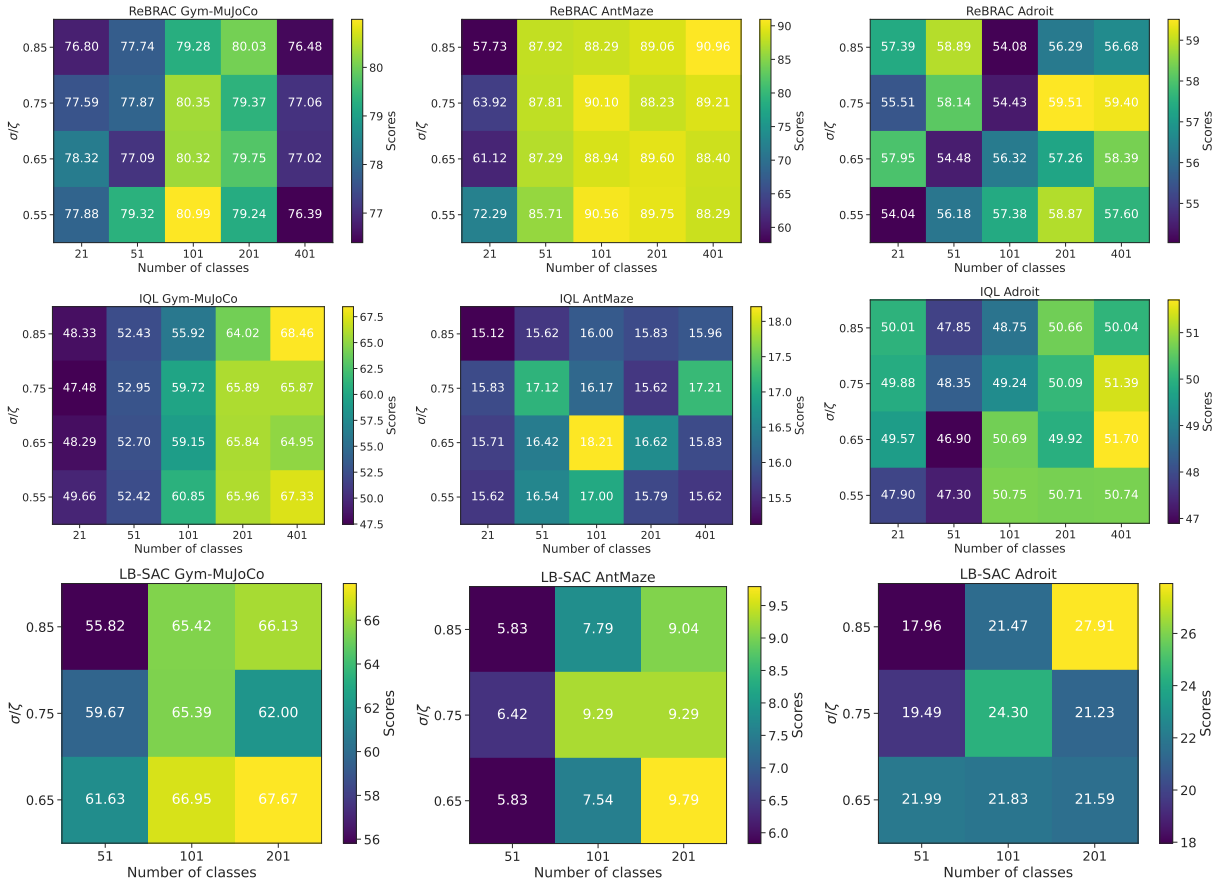

Figure 1: Heatmaps for the impact of the classification parameters averaged over the domains. See Appendix I and Appendix E for more results.

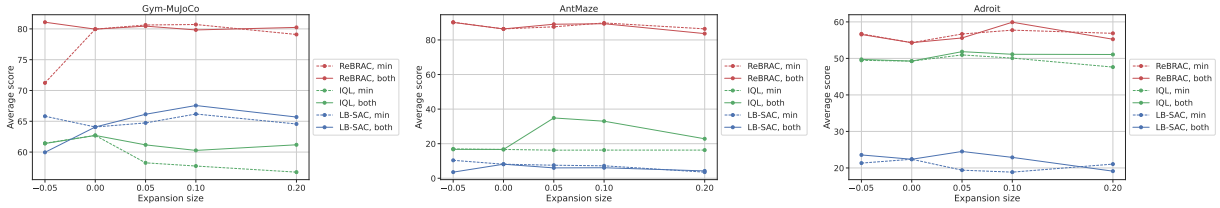

Figure 2: Dependency of the algorithms performance on v_{expand} values averaged over domains. See Appendix F for tabular representation.

in the development of novel RL approaches. Experimental results are presented in Figure 3. Surprisingly, our findings suggest that there is no consistent improvement in terms of scaling when MSE is replaced with cross-entropy.

This discrepancy from the results reported by Farebrother et al. (2024) could be attributed to the fundamental architectural differences between MLPs and models like Transformers or ResNets. Unlike these latter architectures, vanilla MLPs typically lack residual connections (He et al., 2016), which have been identified as a crucial factor in enabling effective scaling with depth. Consequently, the absence of such connections in MLPs may limit their ability to capitalize on the benefits offered by classification over regression.

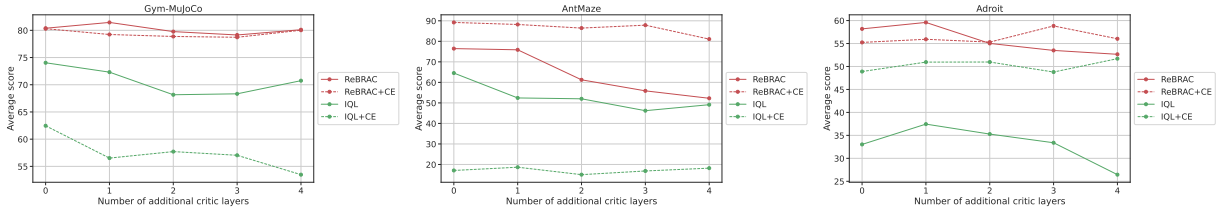

Figure 3: Dependency of the algorithms performance on the number of additional layers averaged over domains. See Appendix D for tabular representation.

4.6 Combining the findings

We investigated whether a mixed tuning strategy for hyperparameters could enhance classification performance, building on our previous findings. For each algorithm, we tuned the following parameters: m from the set $\{201, 401\}$, v_{expand} from the set of $\{-0.05, 0.05, 0.1\}$ using the *both* strategy, and three values for one of algorithm-specific parameter: β_1 for ReBRAC, IQL τ for IQL, and N critics for LB-SAC. For ReBRAC and IQL, the second parameter was held constant across all tasks (see subsection A.1). σ/ζ was set to 0.75. To enhance readability, we provide detailed per-dataset results in a separate tables in Appendix G and EOP results in Table 4 under the **+CE+MT** rows (see also Appendix H).

Per-dataset results indicate that the proposed strategy yields better performance in most cases, performing on par in others, with the exception of LB-SAC on Gym-MuJoCo. It makes this approach the best choice when no prior knowledge on optimal algorithm-specific parameters is available.

EOP results reveal that this tuning strategy is particularly effective for IQL, especially under a low fine-tuning budget. For ReBRAC, benefits are apparent only under a high fine-tuning budget. Conversely, this strategy did not perform well for LB-SAC. The suboptimal performance of LB-SAC can be attributed to the strong dependence on ensemble size; due to computational constraints, we were unable to use an ensemble size of 50, which is optimal for many datasets.

To conclude, our experiments show that the best performance with classification can be achieved by tuning algorithm-specific hyperparameters in conjunction with classification parameters, particularly the support range and the number of bins.

4.7 Learned Q-functions analysis

Finally, in Figure 4 we present the dynamics of the Q-function learning for ReBRAC and IQL on AntMaze datasets, as they are of the most interest based on our results. For ReBRAC, modified versions have lower Q-function values on average, but the learning pattern remains similar, except for **CE+MT**, where the Q-values are notably lower, and the shape of the curve is different. However, these differences in the Q-function between **CE+MT** and **CE+AT**/**CE+CT** do not result in significant differences in average performance. For IQL, the plots demonstrate that the usage of classification leads to more optimistic Q-functions, with a significant gap between MSE and others. Unfortunately, there is no consistent pattern. We cannot claim that a more optimistic Q-function is the core issue for IQL because, for example, **CE+MT** is sometimes above **CE+CT**, but this has no correlation with task performance.

5 Related Work

Prior research beyond the realm of RL has demonstrated the potential performance enhancements associated with replacing regression with classification objectives (Van Den Oord et al., 2016; Kendall et al., 2017; Rothe et al., 2018; Rogez et al., 2017). Within the RL domain, some studies have experimented with employing classification objectives as a workaround, albeit without conducting comprehensive analyses of this modification (Schrittwieser et al., 2020; Hafner et al., 2023; Hessel et al., 2021; Hansen et al., 2023). Categorical distributional RL (Bellemare et al., 2017) works are also relevant for the considered topic, where

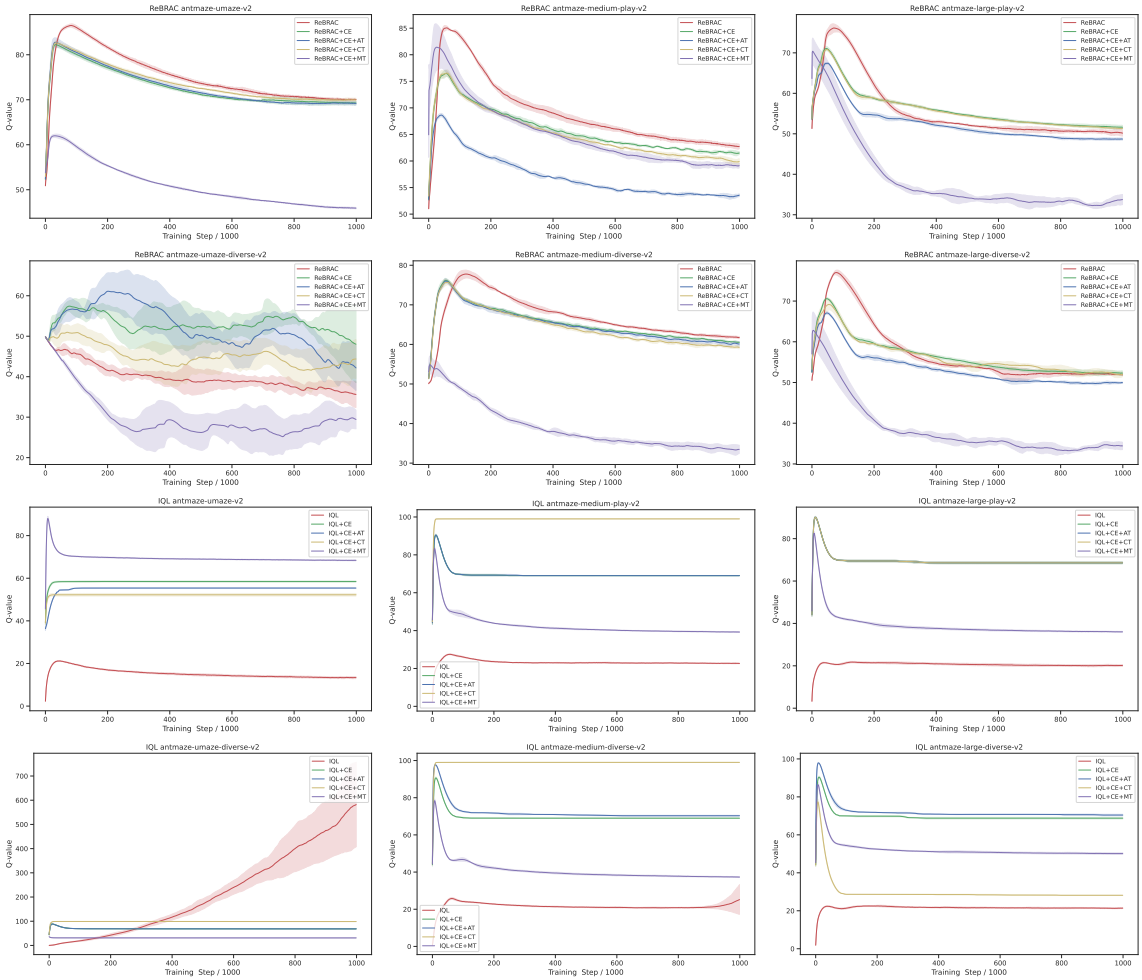

Figure 4: Q-value functions behaviour for ReBRAC and IQL on AntMaze tasks. Shaded area demonstrates standard deviation across ten random seeds.

the classification is also used, however usage of classification instead of regression is not a central topic in this reseach direction. Additionally, several works in offline RL have demonstrated the benefits of utilizing classification objectives for various tasks, albeit lacking in-depth analyses of this specific component and its elements (Kumar et al., 2022; Springenberg et al., 2024).

To the best of our knowledge, (Farebrother et al., 2024) represent the first and only study to make regression replacement with classification a central research question. The authors compared different methods of converting regression targets into classification targets, providing experimental results across a diverse array of tasks encompassing Atari games, robotics, and natural language processing problems in online and offline RL setups. Their study revealed that HL-Gauss (Imani & White, 2018) represents the optimal approach for representing RL regression targets with categorical distributions while this was not the case for the supervised regression tasks (Imani & White, 2018). The authors assert that cross-entropy serves as a "drop-in" replacement for MSE in RL, leading to a more stable training process and enhanced scalability with deep neural network architectures such as Transformers (Vaswani et al., 2017) or ResNets (He et al., 2016). Our work draws primary inspiration from (Farebrother et al., 2024) and aims to provide a more in-depth analysis of this phenomenon in offline RL, which we believe holds significant potential benefits for both offline RL researchers and practitioners.

6 Conclusion

In this study, we explored the impact of integrating classification objectives into offline RL algorithms. Our findings provide nuanced insights into the efficacy of classification in improving offline RL algorithm performance. Initially, we examined whether classification objectives could be seamlessly integrated into existing algorithms without altering other aspects. While some algorithm with policy regularization (ReBRAC) demonstrated promising results across various tasks , other algorithms with implicit regularization (IQL) and algorithm with Q function regularization (LB-SAC) faced challenges. And the only case when classification have high chances to bring improvement without much effort is the divergence of Q function with MSE loss.

Next, we explored the impact of different hyperparameter tuning with classification objectives. Notably, we observed performance improvements for ReBRAC, when tuning classification hyperparameters over algorithm-specific ones. Other results underscore the importance of carefully selecting both types of hyperparameters: algorithm-specific and classification-specific, when employing classification.

Furthermore, our investigation into the scalability of MLPs with classification revealed mixed results. Contrary to previous findings with architectures like Transformers and ResNets, we did not observe consistent improvements in scaling when using classification objectives with MLPs. This highlights the importance of considering the architectural nuances of different models when assessing the potential benefits of classification objectives.

Looking ahead, several avenues for future research emerge. One promising direction involves examining how classification affects the performance of offline algorithms in offline-to-online RL setup. Understanding how classification objectives impact the transferability of learned policies to online settings could provide valuable insights into the practical applicability of classification usage. Another theoretically promising direction is leveraging classification-specifics for uncertainty estimation in offline RL. For example, the entropy provided by the Q function could be used to incorporate pessimism into offline RL algorithms.

In conclusion, our study underscores the need for a nuanced understanding of the interplay between algorithm design, task characteristics, and the integration of classification objectives in RL. While classification holds promise in certain contexts, its efficacy is highly dependent on factors such as algorithm design and hyperparameter selection. Future research could further explore these nuances and develop approaches that leverage classification objectives optimally across a diverse range of RL tasks and algorithms.

References

Rishabh Agarwal, Max Schwarzer, Pablo Samuel Castro, Aaron C Courville, and Marc Bellemare. Deep reinforcement learning at the edge of the statistical precipice. *Advances in neural information processing systems*, 34:29304–29320, 2021.

Dmitriy Akimov, Vladislav Kurenkov, Alexander Nikulin, Denis Tarasov, and Sergey Kolesnikov. Let offline rl flow: Training conservative agents in the latent space of normalizing flows. *arXiv preprint arXiv:2211.11096*, 2022.

Gaon An, Seungyong Moon, Jang-Hyun Kim, and Hyun Oh Song. Uncertainty-based offline reinforcement learning with diversified q-ensemble. *Advances in neural information processing systems*, 34:7436–7447, 2021.

Marc G Bellemare, Will Dabney, and Rémi Munos. A distributional perspective on reinforcement learning. In *International conference on machine learning*, pp. 449–458. PMLR, 2017.

Lili Chen, Kevin Lu, Aravind Rajeswaran, Kimin Lee, Aditya Grover, Misha Laskin, Pieter Abbeel, Aravind Srinivas, and Igor Mordatch. Decision transformer: Reinforcement learning via sequence modeling. *Advances in neural information processing systems*, 34:15084–15097, 2021.

Xi Chen, Ali Ghadirzadeh, Tianhe Yu, Yuan Gao, Jianhao Wang, Wenzhe Li, Bin Liang, Chelsea Finn, and Chongjie Zhang. Latent-variable advantage-weighted policy optimization for offline rl. *arXiv preprint arXiv:2203.08949*, 2022.

Jesse Farebrother, Jordi Orbay, Quan Vuong, Adrien Ali Taïga, Yevgen Chebotar, Ted Xiao, Alex Irpan, Sergey Levine, Pablo Samuel Castro, Aleksandra Faust, et al. Stop regressing: Training value functions via classification for scalable deep rl. *arXiv preprint arXiv:2403.03950*, 2024.

Justin Fu, Aviral Kumar, Ofir Nachum, George Tucker, and Sergey Levine. D4rl: Datasets for deep data-driven reinforcement learning. *arXiv preprint arXiv:2004.07219*, 2020.

Scott Fujimoto and Shixiang Shane Gu. A minimalist approach to offline reinforcement learning. *Advances in neural information processing systems*, 34:20132–20145, 2021.

Kamyar Ghasemipour, Shixiang Shane Gu, and Ofir Nachum. Why so pessimistic? estimating uncertainties for offline rl through ensembles, and why their independence matters. *Advances in Neural Information Processing Systems*, 35:18267–18281, 2022.

Danijar Hafner, Jurgis Pasukonis, Jimmy Ba, and Timothy Lillicrap. Mastering diverse domains through world models. *arXiv preprint arXiv:2301.04104*, 2023.

Nicklas Hansen, Hao Su, and Xiaolong Wang. Td-mpc2: Scalable, robust world models for continuous control. *arXiv preprint arXiv:2310.16828*, 2023.

Kaiming He, Xiangyu Zhang, Shaoqing Ren, and Jian Sun. Deep residual learning for image recognition. In *Proceedings of the IEEE conference on computer vision and pattern recognition*, pp. 770–778, 2016.

Matteo Hessel, Ivo Danihelka, Fabio Viola, Arthur Guez, Simon Schmitt, Laurent Sifre, Theophane Weber, David Silver, and Hado Van Hasselt. Muesli: Combining improvements in policy optimization. In *International conference on machine learning*, pp. 4214–4226. PMLR, 2021.

Ehsan Imani and Martha White. Improving regression performance with distributional losses. In *International conference on machine learning*, pp. 2157–2166. PMLR, 2018.

Ehsan Imani, Kai Luedemann, Sam Scholnick-Hughes, Esraa Elelimy, and Martha White. Investigating the histogram loss in regression. *arXiv preprint arXiv:2402.13425*, 2024.

Alex Kendall, Hayk Martirosyan, Saumitro Dasgupta, Peter Henry, Ryan Kennedy, Abraham Bachrach, and Adam Bry. End-to-end learning of geometry and context for deep stereo regression. In *Proceedings of the IEEE international conference on computer vision*, pp. 66–75, 2017.

Diederik P Kingma and Jimmy Ba. Adam: A method for stochastic optimization. *arXiv preprint arXiv:1412.6980*, 2014.

Ilya Kostrikov, Ashvin Nair, and Sergey Levine. Offline reinforcement learning with implicit q-learning. *arXiv preprint arXiv:2110.06169*, 2021.

Aviral Kumar, Rishabh Agarwal, Dibya Ghosh, and Sergey Levine. Implicit under-parameterization inhibits data-efficient deep reinforcement learning. *arXiv preprint arXiv:2010.14498*, 2020a.

Aviral Kumar, Aurick Zhou, George Tucker, and Sergey Levine. Conservative q-learning for offline reinforcement learning. *Advances in Neural Information Processing Systems*, 33:1179–1191, 2020b.

Aviral Kumar, Rishabh Agarwal, Tengyu Ma, Aaron Courville, George Tucker, and Sergey Levine. Dr3: Value-based deep reinforcement learning requires explicit regularization. *arXiv preprint arXiv:2112.04716*, 2021.

Aviral Kumar, Rishabh Agarwal, Xinyang Geng, George Tucker, and Sergey Levine. Offline q-learning on diverse multi-task data both scales and generalizes. *arXiv preprint arXiv:2211.15144*, 2022.

Vladislav Kurenkov and Sergey Kolesnikov. Showing your offline reinforcement learning work: Online evaluation budget matters. In *International Conference on Machine Learning*, pp. 11729–11752. PMLR, 2022.

Sergey Levine, Aviral Kumar, George Tucker, and Justin Fu. Offline reinforcement learning: Tutorial, review, and perspectives on open problems. *arXiv preprint arXiv:2005.01643*, 2020.

Clare Lyle, Mark Rowland, and Will Dabney. Understanding and preventing capacity loss in reinforcement learning. *arXiv preprint arXiv:2204.09560*, 2022.

Alexander Nikulin, Vladislav Kurenkov, Denis Tarasov, Dmitry Akimov, and Sergey Kolesnikov. Q-ensemble for offline rl: Don't scale the ensemble, scale the batch size. *arXiv preprint arXiv:2211.11092*, 2022.

Alexander Nikulin, Vladislav Kurenkov, Denis Tarasov, and Sergey Kolesnikov. Anti-exploration by random network distillation. *arXiv preprint arXiv:2301.13616*, 2023.

Gregory Rogez, Philippe Weinzaepfel, and Cordelia Schmid. Lcr-net: Localization-classification-regression for human pose. In *Proceedings of the IEEE conference on computer vision and pattern recognition*, pp. 3433–3441, 2017.

Gregory Rogez, Philippe Weinzaepfel, and Cordelia Schmid. Lcr-net++: Multi-person 2d and 3d pose detection in natural images. *IEEE transactions on pattern analysis and machine intelligence*, 42(5): 1146–1161, 2019.

Rasmus Rothe, Radu Timofte, and Luc Van Gool. Deep expectation of real and apparent age from a single image without facial landmarks. *International Journal of Computer Vision*, 126(2):144–157, 2018.

Julian Schrittwieser, Ioannis Antonoglou, Thomas Hubert, Karen Simonyan, Laurent Sifre, Simon Schmitt, Arthur Guez, Edward Lockhart, Demis Hassabis, Thore Graepel, et al. Mastering atari, go, chess and shogi by planning with a learned model. *Nature*, 588(7839):604–609, 2020.

David Silver, Julian Schrittwieser, Karen Simonyan, Ioannis Antonoglou, Aja Huang, Arthur Guez, Thomas Hubert, Lucas Baker, Matthew Lai, Adrian Bolton, et al. Mastering the game of go without human knowledge. *nature*, 550(7676):354–359, 2017.

Jost Tobias Springenberg, Abbas Abdolmaleki, Jingwei Zhang, Oliver Groth, Michael Bloesch, Thomas Lampe, Philemon Brakel, Sarah Bechtle, Steven Kapturowski, Roland Hafner, et al. Offline actor-critic reinforcement learning scales to large models. *arXiv preprint arXiv:2402.05546*, 2024.

Lawrence Stewart, Francis Bach, Quentin Berthet, and Jean-Philippe Vert. Regression as classification: Influence of task formulation on neural network features. In *International Conference on Artificial Intelligence and Statistics*, pp. 11563–11582. PMLR, 2023.

Denis Tarasov, Vladislav Kurenkov, Alexander Nikulin, and Sergey Kolesnikov. Revisiting the minimalist approach to offline reinforcement learning. *Advances in Neural Information Processing Systems*, 36, 2024a.

Denis Tarasov, Alexander Nikulin, Dmitry Akimov, Vladislav Kurenkov, and Sergey Kolesnikov. Corl: Research-oriented deep offline reinforcement learning library. *Advances in Neural Information Processing Systems*, 36, 2024b.

Aäron Van Den Oord, Nal Kalchbrenner, and Koray Kavukcuoglu. Pixel recurrent neural networks. In *International conference on machine learning*, pp. 1747–1756. PMLR, 2016.

Ashish Vaswani, Noam Shazeer, Niki Parmar, Jakob Uszkoreit, Llion Jones, Aidan N Gomez, Łukasz Kaiser, and Illia Polosukhin. Attention is all you need. *Advances in neural information processing systems*, 30, 2017.

Rui Yang, Chenjia Bai, Xiaoteng Ma, Zhaoran Wang, Chongjie Zhang, and Lei Han. Rorl: Robust offline reinforcement learning via conservative smoothing. *Advances in Neural Information Processing Systems*, 35:23851–23866, 2022.

Shihao Zhang, Linlin Yang, Michael Bi Mi, Xiaoxu Zheng, and Angela Yao. Improving deep regression with ordinal entropy. *arXiv preprint arXiv:2301.08915*, 2023.

A Experimental Details

For results with original algorithms and algorithms hyperparameters search in Table 1 Table 2 and Table 3, we conducted a hyperparameter search and selected the best results from the final evaluations for each dataset. We used the JAX implementation of ReBRAC from the Clean Offline RL (CORL) library (Tarasov et al., 2024b) and used the same code template for IQL and LB-SAC. Algorithmic part of IQL implementation is based on the original codebase from Kostrikov et al. (2021) and in case of LB-SAC we have adapted SAC-N implementation from `https://github.com/Howuhh/sac-n-jax`.

The experiments were conducted on RTX Titan, Quadro RTX 6000 and Quadro RTX 8000.

Our study utilized the v2 version of datasets for Gym-MuJoCo and AntMaze, and v1 for Adroit. The agents were trained for one million steps in all domains and evaluated over ten episodes for Gym-MuJoCo and Adroit and over one hundred episodes for AntMaze. Following Chen et al. (2022), AntMaze reward function is multiplied by 100.

For ReBRAC, we fine-tuned the β_1 parameter with $0.001, 0.01, 0.05, 0.1$ values and the β_2 parameter with $0, 0.001, 0.01, 0.1, 0.5$ values for Gym-MuJoCo and Adroit. For AntMaze the corresponding ranges are $0.0005, 0.001, 0.002, 0.003$ and $0, 0.0001, 0.0005, 0.001$. When replacing regression with classification for AntMaze we also set batch size to 1024 and learning rates to 0.001 as it is was done for Gym-MuJoCo in original algorithm which slightly improves the performance.

For IQL in all domains, we selected β value from $0.5, 1, 3, 6, 10$ and IQL τ from $0.5, 0.7, 0.9, 0.95$.

For LB-SAC we selected the number of critics in the range of $2, 5, 10, 25, 50$. Note, that for LB-SAC we used sub-optimal parameters of the batch size and learning rate due to the computational constraints.

A.1 Mixed tuning hyperparameters choice

For ReBRAC, we fine-tuned the β_1 parameter with $0.001, 0.01, 0.05$ values and the β_2 parameter was set to 0.001.

For IQL, we selected IQL τ from $0.5, 0.7, 0.9$ and set β value to 3.

For LB-SAC we selected the number of critics in the range of $2, 10, 25$.

B Hyperparameters

B.1 ReBRAC

Table 5: ReBRAC's general hyperparameters.

Parameter	**Value**
optimizer	Adam Kingma & Ba (2014)
batch size	1024 on Gym-MuJoCo and AntMaze (for classification), 256 otherwise
learning rate (all networks)	1e-3 on Gym-MuJoCo and AntMaze (for classification), 3e-4 otherwise
tau (τ)	5e-3
hidden dim (all networks)	256
num hidden layers (all networks)	3
gamma (γ)	0.999 on AntMaze, 0.99 otherwise
nonlinearity	ReLU

Table 6: ReBRAC's best hyperparameters.

Task Name	β_1 (MSE)	β_2 (MSE)	β_1 (CE+AT)	β_2 (CE+AT)	m (CE+CT)	σ/ζ (CE+CT)	β_1 (CE+MT)	m (CE+MT)	v_{expand} (CE+MT)
halfcheetah-random	0.001	0.1	0.001	0.1	101	0.85	0.001	201	0.05
halfcheetah-medium	0.001	0.01	0.001	0.5	21	0.75	0.001	201	0.1
halfcheetah-expert	0.01	0.01	0.01	0.01	201	0.85	0.01	201	0.05
halfcheetah-medium-expert	0.01	0.1	0.01	0.001	101	0.85	0.01	201	0.1
halfcheetah-medium-replay	0.01	0.001	0.001	0.001	201	0.65	0.001	201	0.1
halfcheetah-full-replay	0.001	0.1	0.001	0.001	21	0.75	0.001	201	-0.05
hopper-random	0.001	0.01	0.001	0.5	201	0.85	0.001	401	-0.05
hopper-medium	0.01	0.001	0.01	0.001	201	0.75	0.01	201	-0.05
hopper-expert	0.1	0.001	0.1	0.1	401	0.65	0.05	401	0.1
hopper-medium-expert	0.1	0.01	0.1	0.0	101	0.75	0.05	401	0.05
hopper-medium-replay	0.05	0.5	0.05	0.0	101	0.75	0.01	401	-0.05
hopper-full-replay	0.01	0.01	0.01	0.0	101	0.65	0.01	201	0.05
walker2d-random	0.01	0.0	0.05	0.1	101	0.65	0.05	201	0.05
walker2d-medium	0.05	0.1	0.05	0.1	101	0.55	0.05	201	0.1
walker2d-expert	0.01	0.5	0.01	0.5	101	0.75	0.01	401	0.05
walker2d-medium-expert	0.01	0.01	0.01	0.5	401	0.85	0.05	401	0.05
walker2d-medium-replay	0.05	0.01	0.05	0.0	201	0.65	0.01	401	-0.05
walker2d-full-replay	0.01	0.01	0.001	0.001	201	0.55	0.001	201	0.1
antmaze-umaze	0.003	0.002	0.003	0.0	401	0.75	0.05	401	0.1
antmaze-umaze-diverse	0.003	0.001	0.003	0.002	201	0.75	0.01	201	0.1
antmaze-medium-play	0.001	0.0005	0.003	0.0005	201	0.65	0.001	401	0.05
antmaze-medium-diverse	0.001	0.0	0.003	0.002	201	0.85	0.01	401	0.1
antmaze-large-play	0.002	0.001	0.003	0.0005	101	0.75	0.01	401	0.1
antmaze-large-diverse	0.002	0.002	0.003	0.0005	401	0.75	0.01	401	0.1
pen-human	0.1	0.5	0.1	0.001	51	0.85	0.05	201	-0.05
pen-cloned	0.05	0.5	0.1	0.001	401	0.75	0.05	401	0.05
pen-expert	0.01	0.01	0.01	0.0	401	0.85	0.01	401	-0.05
door-human	0.1	0.1	0.1	0.1	401	0.85	0.001	401	-0.05
door-cloned	0.01	0.1	0.1	0.001	101	0.55	0.05	201	0.1
door-expert	0.05	0.01	0.05	0.001	401	0.75	0.05	401	-0.05
hammer-human	0.01	0.5	0.1	0.001	51	0.85	0.05	201	-0.05
hammer-cloned	0.1	0.5	0.05	0.1	21	0.85	0.05	401	0.05
hammer-expert	0.01	0.01	0.01	0.5	401	0.55	0.01	401	0.1
relocate-human	0.1	0.01	0.1	0.01	201	0.55	0.05	201	0.05
relocate-cloned	0.1	0.01	0.1	0.0	401	0.75	0.05	201	0.1
relocate-expert	0.05	0.01	0.05	0.5	21	0.55	0.05	401	0.05

B.2 IQL

Table 7: IQL's general hyperparameters.

Parameter	**Value**
optimizer	Adam Kingma & Ba (2014)
batch size	256
learning rate (all networks)	3e-4
tau (τ)	5e-3
hidden dim (all networks)	256
num hidden layers (all networks)	2
gamma (γ)	0.99
nonlinearity	ReLU
learning rate decay	Cosine
dropout rate	0.1 for Adroit, 0 otherwise

Table 8: IQL's best hyperparameters.

Task Name	IQL τ (MSE)	β (MSE)	IQL τ (CE+AT)	β (CE+AT)	m (CE+CT)	σ/ζ (CE+CT)	IQL τ (CE+MT)	m (CE+MT)	v_{expand} (CE+MT)
halfcheetah-random	0.95	10.0	0.5	3.0	401	0.55	0.7	401	-0.05
halfcheetah-medium	0.95	3.0	0.5	10.0	401	0.55	0.7	401	0.1
halfcheetah-expert	0.7	6.0	0.7	1.0	401	0.55	0.5	401	0.1
halfcheetah-medium-expert	0.5	0.5	0.5	3.0	401	0.75	0.7	401	0.1
halfcheetah-medium-replay	0.9	6.0	0.5	6.0	401	0.55	0.7	401	0.1
halfcheetah-full-replay	0.5	0.5	0.5	6.0	401	0.55	0.5	401	0.1
hopper-random	0.95	10.0	0.95	6.0	51	0.85	0.9	201	-0.05
hopper-medium	0.7	0.5	0.7	10.0	51	0.85	0.5	201	0.05
hopper-expert	0.9	0.5	0.7	3.0	201	0.75	0.9	201	-0.05
hopper-medium-expert	0.7	10.0	0.5	3.0	201	0.85	0.5	401	0.05
hopper-medium-replay	0.7	0.5	0.5	6.0	401	0.85	0.7	401	0.05
hopper-full-replay	0.7	3.0	0.5	3.0	401	0.55	0.5	401	-0.05
walker2d-random	0.9	0.5	0.95	3.0	21	0.65	0.9	401	0.1
walker2d-medium	0.5	1.0	0.5	0.5	101	0.55	0.7	401	0.1
walker2d-expert	0.7	6.0	0.7	10.0	401	0.55	0.7	401	0.05
walker2d-medium-expert	0.7	3.0	0.5	6.0	401	0.85	0.5	401	0.1
walker2d-medium-replay	0.7	1.0	0.5	6.0	401	0.75	0.7	401	0.05
walker2d-full-replay	10.0	0.7	0.5	1.0	401	0.55	0.7	401	0.1
antmaze-umaze	0.7	10.0	0.5	3.0	101	0.65	0.9	201	0.05
antmaze-umaze-diverse	0.9	10.0	0.9	6.0	51	0.75	0.5	201	0.05
antmaze-medium-play	0.9	6.0	0.9	1.0	51	0.75	0.9	401	0.1
antmaze-medium-diverse	0.9	6.0	0.95	6.0	51	0.75	0.9	401	0.1
antmaze-large-play	0.9	10.0	0.9	10.0	101	0.75	0.9	401	0.1
antmaze-large-diverse	0.9	6.0	0.95	3.0	201	0.55	0.9	201	0.05
pen-human	0.7	0.5	0.7	1.0	201	0.85	0.9	201	-0.05
pen-cloned	0.9	10.0	0.5	0.5	401	0.65	0.5	401	0.1
pen-expert	0.9	0.5	0.5	10.0	401	0.75	0.5	401	-0.05
door-human	0.95	1.0	0.9	6.0	401	0.75	0.9	201	0.1
door-cloned	0.7	1.0	0.9	0.5	21	0.75	0.7	201	0.1
door-expert	0.9	10.0	0.9	6.0	101	0.55	0.7	201	0.05
hammer-human	0.9	10.0	0.7	3.0	21	0.55	0.7	401	-0.05
hammer-cloned	0.7	6.0	0.7	10.0	21	0.65	0.7	201	0.1
hammer-expert	0.95	0.5	0.95	0.5	401	0.65	0.9	401	-0.05
relocate-human	0.7	10.0	0.7	1.0	101	0.75	0.9	401	0.05
relocate-cloned	0.7	1.0	0.7	1.0	201	0.65	0.9	401	0.05
relocate-expert	0.5	0.5	0.95	0.5	401	0.75	0.9	401	0.1

B.3 LB-SAC

Table 9: LB-SAC's general hyperparameters.

Parameter	**Value**
optimizer	Adam Kingma & Ba (2014)
batch size	1024
learning rate (all networks)	6e-4
tau (τ)	5e-3
hidden dim (all networks)	256
num hidden layers (all networks)	3
gamma (γ)	0.99
nonlinearity	ReLU

Table 10: LB-SAC's best hyperparameters.

Task Name	N critics (MSE)	N critics (CE+AT)	m (CE+CT)	σ/ζ (CE+CT)	N critics (CE+MT)	m (CE+MT)	v_{expand} (CE+MT)
halfcheetah-random	2	50	51	0.75	2	201	0.1
halfcheetah-medium	2	5	101	0.75	10	201	-0.05
halfcheetah-expert	5	5	51	0.85	10	201	0.05
halfcheetah-medium-expert	5	5	201	0.85	10	201	-0.05
halfcheetah-medium-replay	5	5	201	0.85	10	201	0.1
halfcheetah-full-replay	2	2	201	0.75	2	401	-0.05
hopper-random	5	25	201	0.85	25	401	-0.05
hopper-medium	25	25	201	0.75	25	401	0.1
hopper-expert	50	50	201	0.65	25	401	0.05
hopper-medium-expert	50	50	51	0.75	25	201	0.1
hopper-medium-replay	5	5	101	0.85	10	201	0.05
hopper-full-replay	5	5	51	0.75	10	201	0.05
walker2d-random	50	5	51	0.75	10	201	0.05
walker2d-medium	10	10	101	0.85	10	201	-0.05
walker2d-expert	25	50	201	0.65	25	401	-0.05
walker2d-medium-expert	10	25	201	0.85	10	401	0.05
walker2d-medium-replay	5	5	101	0.85	10	201	0.1
walker2d-full-replay	5	5	201	0.85	10	201	0.1
antmaze-umaze	5	5	201	0.65	2	201	0.1
antmaze-umaze-diverse	25	2	101	0.75	2	401	0.05
antmaze-medium-play	25	5	101	0.75	2	401	0.05
antmaze-medium-diverse	25	5	101	0.75	2	401	0.05
antmaze-large-play	25	25	101	0.75	25	201	0.1
antmaze-large-diverse	25	25	101	0.75	25	201	0.1
pen-human	5	10	51	0.75	10	201	0.05
pen-cloned	50	50	51	0.65	25	201	-0.05
pen-expert	25	25	201	0.85	25	201	0.1
door-human	2	50	51	0.75	25	201	0.05
door-cloned	50	50	201	0.85	25	201	0.05
door-expert	50	50	201	0.75	25	401	0.05
hammer-human	5	50	101	0.75	2	201	-0.05
hammer-cloned	50	25	51	0.85	10	201	-0.05
hammer-expert	25	25	201	0.85	10	401	0.05
relocate-human	2	50	101	0.65	25	401	0.1
relocate-cloned	50	50	101	0.85	25	201	-0.05
relocate-expert	50	25	101	0.75	25	401	-0.05

C Computational Costs

Table 11: Computational costs for all experiments. Note, ReBRAC computational costs are taken from Tarasov et al. (2024a). The total amount of compute is approximately 23497 hours (979 days).

Algorithm	**Number of runs**	**Approximate hours per run**
ReBRAC+MSE, tuning	2784	0.39
ReBRAC+CE+AT, tuning	2784	0.34
ReBRAC+CE+CT, tuning	2880	0.48
ReBRAC+CE+MT, tuning	2592	0.50
IQL+MSE, tuning	2880	0.3
IQL+CE+AT, tuning	2880	0.26
IQL+CE+CT, tuning	2880	0.27
IQL+CE+MT, tuning	2592	0.30
LB-SAC+MSE, tuning	720	1.29
LB-SAC+CE+AT, tuning	720	1.61
LB-SAC+CE+CT, tuning	1296	2.32
LB-SAC+CE+MT, tuning	2592	1.56
ReBRAC+MSE, eval	360	0.36
ReBRAC+CE, eval	144	0.45
ReBRAC+CE+AT, eval	144	0.47
ReBRAC+CE+CT, eval	144	0.47
ReBRAC+CE+MT, eval	144	0.34
IQL+MSE, eval	144	0.35
IQL+CE, eval	144	0.33
IQL+CE+AT, eval	144	0.24
IQL+CE+CT, eval	144	0.34
IQL+CE+MT, eval	144	0.34
LB-SAC+MSE, eval	144	1.25
LB-SAC+CE, eval	144	1.34
LB-SAC+CE+AT, eval	144	1.69
LB-SAC+CE+CT, eval	144	2.21
LB-SAC+CE+MT, eval	144	1.89
ReBRAC+MSE, depth scale	720	0.61
ReBRAC+CE, depth scale	720	0.38
IQL+MSE, depth scale	720	0.35
IQL+CE, depth scale	720	0.38
ReBRAC, v_{expand}	1440	0.45
IQL+CE, v_{expand}	1440	0.34
LB-SAC+CE, v_{expand}	1440	2.53
Sum (w/o ReBRAC MSE)	34032	0.69

D MLPs Scale

Table 12: Dependency of the algorithms performance on the number of additional layers averaged over domains.

Domain	Algorithm	+0 layers	+1 layer	+2 layers	+3 layers	+4 layers
Gym-MuJoCo	**ReBRAC**	80.3	81.4	79.7	79.1	80.1
	ReBRAC+CE	80.3	79.2	78.8	78.7	80.0
	IQL	74.0	72.3	68.1	68.3	70.7
	IQL+CE	62.4	56.5	57.7	57.0	53.4
AntMaze	**ReBRAC**	76.4	75.8	61.2	55.8	52.2
	ReBRAC+CE	89.2	88.2	86.4	87.8	81.0
	IQL	64.5	52.4	52.0	46.2	49.1
	IQL+CE	17.0	18.6	15.0	16.8	18.2
Adroit	**ReBRAC**	58.1	59.5	55.0	53.4	52.6
	ReBRAC+CE	55.2	55.9	55.3	58.8	56.0
	IQL	33.0	37.4	35.2	33.3	26.4
	IQL+CE	48.9	50.9	50.9	48.7	51.7

E Impact of m and σ/ζ

Table 13: Average performance on different domains for a fixed m value and averaged over σ/ζ.

Domain	Algorithm	21	51	101	201	401
Gym-MuJoCo	**ReBRAC+CE**	77.6	78.0	80.2	79.5	76.7
	IQL+CE	48.4	52.6	58.9	65.4	66.6
	LB-SAC+CE	-	59.0	65.9	65.2	-
AntMaze	**ReBRAC+CE**	63.7	87.1	89.4	89.1	89.2
	IQL+CE	15.5	16.4	16.8	15.9	16.1
	LB-SAC+CE	-	6.0	8.2	9.3	-
Adroit	**ReBRAC+CE**	56.2	56.9	55.5	57.9	58.0
	IQL+CE	49.3	47.5	49.8	50.3	50.9
	LB-SAC+CE	-	19.8	22.5	23.5	-
Average (w/o LB-SAC)		51.7	56.4	58.4	59.6	59.5
Average		-	47.0	49.6	50.6	-

Table 14: Average performance on different domains for a fixed σ/ζ value and averaged over m.

Domain	Algorithm	0.55	0.65	0.75	0.85
Gym-MuJoCo	**ReBRAC+CE**	78.7	78.4	78.4	78.0
	IQL+CE	59.2	58.1	58.3	57.8
	LB-SAC+CE	-	59.0	65.9	65.2
AntMaze	**ReBRAC+CE**	85.3	83.0	83.8	82.7
	IQL+CE	16.1	16.5	16.3	15.7
	LB-SAC+CE	-	6.0	8.2	9.3
Adroit	**ReBRAC+CE**	56.8	56.8	57.3	56.6
	IQL+CE	49.4	49.7	49.7	49.4
	LB-SAC+CE	-	19.8	22.5	23.5
Average (w/o LB-SAC)		57.5	57.0	57.3	56.7
Average		-	47.4	48.9	48.6

F Impact of v_{min} and v_{max}

Table 15: Dependency of the algorithm's performance on the v_{expand} parameter.

Domain	Algorithm	-0.05	0.0	0.05	0.1	0.2
Gym-MuJoCo	**ReBRAC,** *both*	81.0	79.9	80.4	79.8	80.2
	ReBRAC, *min*	71.2	79.9	80.6	80.7	79.0
	IQL, *both*	61.3	62.7	61.1	60.2	61.1
	IQL, *min*	61.4	62.7	58.2	57.7	56.7
	LB-SAC, *both*	59.9	64.0	66.1	67.5	65.6
	LB-SAC, *min*	65.8	64.0	64.7	66.1	64.5
AntMaze	**ReBRAC,** *both*	90.1	86.3	89.0	89.3	83.6
	ReBRAC, *min*	90.2	86.3	87.5	89.8	86.4
	IQL, *both*	16.7	16.6	34.8	33.0	22.8
	IQL, *min*	16.9	16.6	16.2	16.2	16.2
	LB-SAC, *both*	3.5	8.1	6.0	6.0	4.25
	LB-SAC, *min*	10.3	8.1	7.5	7.2	3.5
Adroit	**ReBRAC,** *both*	56.5	54.3	55.5	59.9	55.2
	ReBRAC, *min*	56.7	54.3	56.6	57.7	56.8
	IQL, *both*	49.7	49.2	51.8	51.1	51.0
	IQL, *min*	49.4	49.2	50.9	50.0	47.6
	LB-SAC, *both*	23.5	22.3	24.5	22.8	19.1
	LB-SAC, *min*	21.3	22.3	19.3	18.8	21.0

G Mixed Tuning Results

Table 16: Average normalized score over the final evaluation and ten (four for LB-SAC) unseen training seeds on Gym-MuJoCo tasks. **CE+MT** denotes cross-entropy with mixed hyperparameters tuning.

	ReBRAC			IQL			LB-SAC		
Task	**MSE**	**CE**	**CE+MT**	**MSE**	**CE**	**CE+MT**	**MSE**	**CE**	**CE+MT**
hc-r	29.5 ± 1.5	13.4 ± 0.8	9.2 ± 0.6	18.9 ± 1.0	1.9 ± 0.0	9.0 ± 3.0	28.2 ± 1.4	10.0 ± 0.3	9.9 ± 0.2
hc-m	65.6 ± 1.0	59.5 ± 0.7	62.0 ± 0.5	49.5 ± 1.1	42.5 ± 0.3	46.8 ± 0.1	64.5 ± 1.3	56.7 ± 2.1	65.5 ± 0.5
hc-e	105.9 ± 1.7	103.2 ± 5.5	104.5 ± 3.1	95.8 ± 2.2	92.9 ± 0.2	94.4 ± 0.3	103.0 ± 1.5	103.9 ± 1.0	98.2 ± 1.6
hc-me	101.1 ± 5.2	103.5 ± 4.3	104.4 ± 2.7	92.3 ± 2.4	86.5 ± 4.0	90.7 ± 3.6	104.5 ± 2.4	105.4 ± 2.0	103.2 ± 2.0
hc-mr	51.0 ± 0.8	50.7 ± 0.7	52.1 ± 5.6	45.2 ± 0.5	38.1 ± 1.8	43.3 ± 0.2	52.8 ± 0.7	55.4 ± 0.9	54.5 ± 1.1
hc-fr	82.1 ± 1.1	83.2 ± 1.5	82.2 ± 1.7	75.5 ± 0.5	62.6 ± 1.1	73.2 ± 0.5	79.0 ± 2.0	80.7 ± 0.3	76.6 ± 9.7
hp-r	8.1 ± 2.4	8.1 ± 0.9	8.5 ± 4.0	6.0 ± 2.8	14.2 ± 2.8	9.5 ± 0.5	14.5 ± 11.5	8.2 ± 2.2	14.8 ± 11.0
hp-m	102.0 ± 1.0	98.9 ± 9.4	102.0 ± 0.4	54.8 ± 4.4	54.1 ± 2.0	50.1 ± 5.8	90.0 ± 27.5	7.9 ± 0.8	15.6 ± 13.5
hp-e	100.1 ± 8.3	107.9 ± 4.9	110.5 ± 0.4	109.4 ± 1.8	110.5 ± 0.5	110.7 ± 0.2	1.3 ± 0.0	21.6 ± 39.7	12.8 ± 12.8
hp-me	107.0 ± 6.4	111.6 ± 0.5	105.4 ± 8.4	88.5 ± 16.5	64.0 ± 10.2	79.4 ± 29.0	111.3 ± 0.3	14.9 ± 7.0	9.1 ± 5.5
hp-mr	98.1 ± 5.3	98.7 ± 3.0	100.2 ± 6.4	95.9 ± 6.4	71.5 ± 10.1	83.7 ± 11.2	63.0 ± 48.1	66.9 ± 42.8	66.7 ± 32.7
hp-fr	107.1 ± 0.4	108.2 ± 0.3	108.5 ± 0.4	107.2 ± 0.6	41.9 ± 4.8	105.7 ± 0.3	107.0 ± 0.7	65.6 ± 50.2	100.3 ± 2.6
wl-r	18.4 ± 4.5	8.8 ± 4.4	7.1 ± 5.4	6.4 ± 6.3	3.9 ± 2.1	9.3 ± 5.7	21.7 ± 0.0	20.1 ± 2.9	21.7 ± 0.1
wl-m	82.5 ± 3.6	85.1 ± 2.7	84.5 ± 2.6	83.2 ± 1.2	79.9 ± 1.3	80.6 ± 4.2	89.3 ± 5.3	89.6 ± 10.7	95.9 ± 3.3
wl-e	112.3 ± 0.2	112.7 ± 0.1	112.3 ± 0.3	113.8 ± 0.2	108.5 ± 0.2	109.5 ± 0.2	114.2 ± 0.4	59.8 ± 45.0	109.8 ± 1.2
wl-me	111.6 ± 0.3	111.7 ± 0.1	110.1 ± 0.2	112.3 ± 0.6	92.2 ± 6.5	110.9 ± 0.3	110.6 ± 0.4	73.1 ± 18.1	111.3 ± 2.5
wl-mr	77.3 ± 7.9	85.2 ± 6.7	83.3 ± 14.7	82.0 ± 7.9	59.1 ± 8.8	83.3 ± 3.0	92.6 ± 2.7	90.9 ± 5.3	84.3 ± 8.9
wl-fr	102.2 ± 1.7	101.8 ± 5.6	100.8 ± 19.5	97.7 ± 1.4	85.3 ± 3.3	93.7 ± 1.1	102.1 ± 1.0	110.4 ± 1.9	95.7 ± 4.0
Avg	81.2	80.6	80.4	74.1	61.6	71.3	74.9	57.8	63.6

Table 17: Average normalized score over the final evaluation and ten (four for LB-SAC) unseen training seeds on AntMaze tasks.

	ReBRAC			IQL			LB-SAC		
Task	**MSE**	**CE**	**CE+MT**	**MSE**	**CE**	**CE+MT**	**MSE**	**CE**	**CE+MT**
um	97.8 ± 1.0	98.0 ± 2.1	97.5 ± 2.0	79.1 ± 6.8	50.0 ± 4.6	80.0 ± 5.2	18.25 ± 35.8	41.0 ± 33.2	61.0 ± 13.7
um-d	88.3 ± 13.0	93.0 ± 4.5	89.0 ± 6.3	72.5 ± 4.5	48.7 ± 6.9	45.8 ± 5.5	0.0 ± 0.0	0.0 ± 0.0	1.0 ± 2.0
med-p	84.0 ± 4.2	88.0 ± 6.3	89.7 ± 5.0	73.8 ± 5.4	0.2 ± 0.4	51.4 ± 10.0	0.0 ± 0.0	0.0 ± 0.0	0.0 ± 0.0
med-d	76.3 ± 13.5	84.8 ± 9.3	89.8 ± 5.4	74.8 ± 3.8	0.4 ± 0.9	43.9 ± 7.1	0.0 ± 0.0	0.0 ± 0.0	8.0 ± 16.0
lrg-p	60.4 ± 26.1	85.9 ± 6.3	86.2 ± 6.6	41.3 ± 7.0	0.0 ± 0.0	11.8 ± 1.9	0.0 ± 0.0	0.0 ± 0.0	0.0 ± 0.0
lrg-d	54.4 ± 25.1	87.1 ± 4.1	80.9 ± 6.8	23.7 ± 5.6	0.0 ± 0.0	4.3 ± 3.1	0.0 ± 0.0	0.0 ± 0.0	0.0 ± 0.0
Avg	76.8	89.4	88.8	60.8	16.5	39.5	3.0	6.8	11.6

Table 18: Average normalized score over the final evaluation and ten (four for LB-SAC) unseen training seeds on Adroit tasks.

	ReBRAC			IQL			LB-SAC		
Task	**MSE**	**CE**	**CE+MT**	**MSE**	**CE**	**CE+MT**	**MSE**	**CE**	**CE+MT**
pen-h	103.5 ± 14.1	102.3 ± 10.2	86.0± 14.5	21.1 ± 16.8	108.2 ± 8.4	105.0 ± 13.3	4.5 ± 2.6	7.1 ± 5.6	6.2 ± 8.5
pen-c	91.8 ± 21.7	90.3 ± 14.2	102.2 ± 20.4	13.2 ± 21.6	12.5 ± 14.7	100.8 ± 11.9	26.1 ± 5.3	20.0 ± 4.5	16.6 ± 8.5
pen-e	154.1 ± 5.4	155.0 ± 5.8	157.9 ± 1.2	60.2 ± 37.7	134.9 ± 7.0	147.0 ± 6.6	130.5 ± 16.8	38.0 ± 13.2	55.3 ± 50.6
door-h	0.0 ± 0.0	0.0 ± 0.0	0.0 ± 0.0	5.9 ± 2.5	4.3 ± 1.0	0.8 ± 0.5	-0.2 ± 0.1	-0.2 ± 0.1	-0.2 ± 0.1
door-c	1.1 ± 2.6	0.0 ± 0.0	0.0 ± 0.0	0.2 ± 0.3	0.3 ± 0.3	6.3 ± 1.8	0.0 ± 0.0	0.2 ± 0.5	0.0 ± 0.0
door-e	104.6 ± 2.4	105.7 ± 1.5	105.7 ± 1.4	105.4 ± 2.0	106.1 ± 0.5	105.8 ± 0.0	95.0 ± 8.6	70.6 ± 33.8	80.6 ± 6.2
ham-h	0.2 ± 0.2	0.1 ± 0.1	2.1 ± 2.7	1.7 ± 0.8	1.5 ± 0.7	3.8 ± 5.2	0.1 ± 0.0	0.0 ± 0.0	0.1 ± 0.0
ham-c	6.7 ± 3.7	9.7 ± 10.4	2.9 ± 2.4	0.2 ± 0.0	1.0 ± 0.7	0.9 ± 0.6	20.2 ± 16.8	13.6 ± 15.4	0.3 ± 0.5
ham-e	133.8 ± 0.7	122.9 ± 19.7	130.5 ± 11.9	129.5 ± 0.2	129.5 ± 0.1	128.8 ± 0.1	76.6 ± 59.5	91.1 ± 10.5	129.3 ± 14.7
rel-h	0.0 ± 0.0	0.0 ± 0.0	0.0 ± 0.2	0.1 ± 0.1	0.1 ± 0.0	0.1 ± 0.0	0.0 ± 0.0	-0.1 ± 0.0	0.0 ± 0.0
rel-c	0.9 ± 1.6	0.4 ± 0.5	0.2 ± 0.2	0.1 ± 0.1	0.1 ± 0.1	0.1 ± 0.1	0.0 ± 0.0	-0.1 ± 0.0	0.0 ± 0.0
rel-e	106.6 ± 3.2	107.8 ± 3.3	108.5 ± 2.2	108.2 ± 0.9	105.7 ± 1.8	110.0 ± 0.7	26.7 ± 18.8	5.3 ± 3.5	0.6 ± 0.2
Avg w/o e	25.5	25.3	24.1	5.3	16.0	27.2	6.3	5.0	2.8
Avg	58.6	57.8	58.0	37.1	50.3	59.1	31.6	20.4	24.0

H rliable Metrics

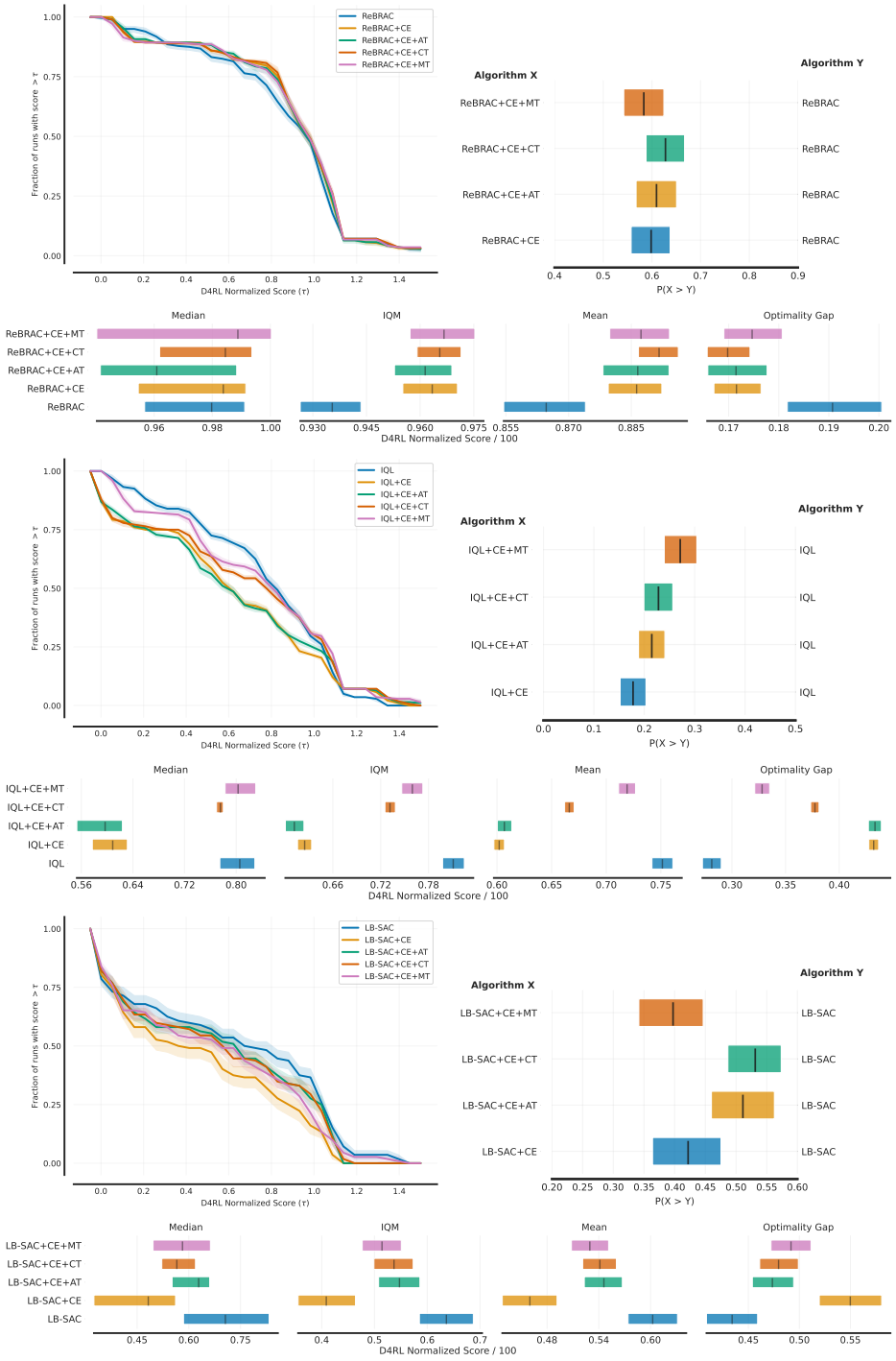

Figure 5: rliable (Agarwal et al., 2021) metrics for ReBRAC, IQL, and LB-SAC averaged over all Gym-MuJoCo, AntMaze and Adroit datasets. Ten evaluation seeds are used for ReBRAC and IQL and four seeds for LB-SAC.

I Classification Parameters Performance Heatmaps

I.1 ReBRAC, Gym-MuJoCo

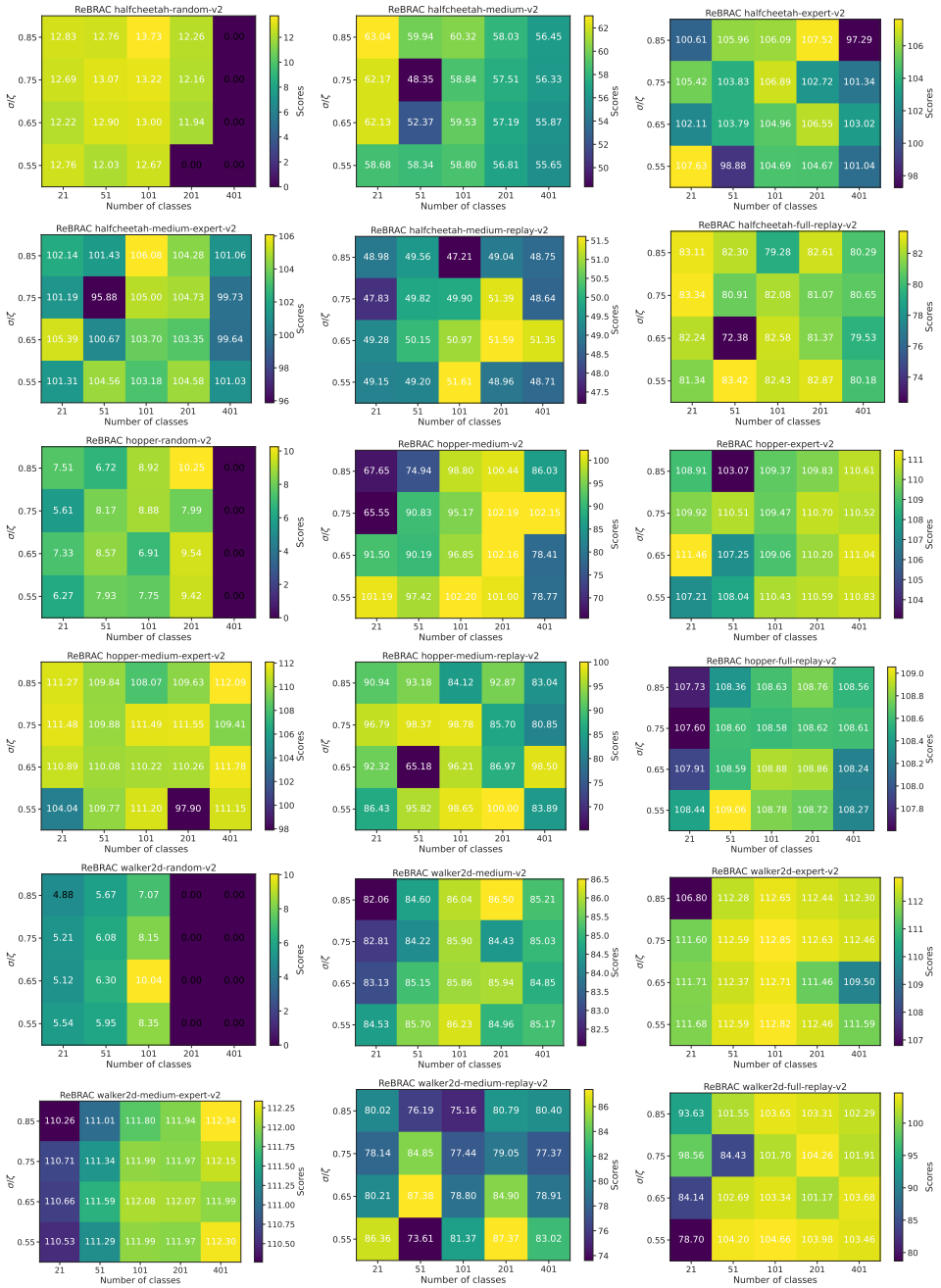

Figure 6: Heatmaps for the impact of the classification parameters on Gym-MuJoCo datasets for ReBRAC.

I.2 ReBRAC, AntMaze

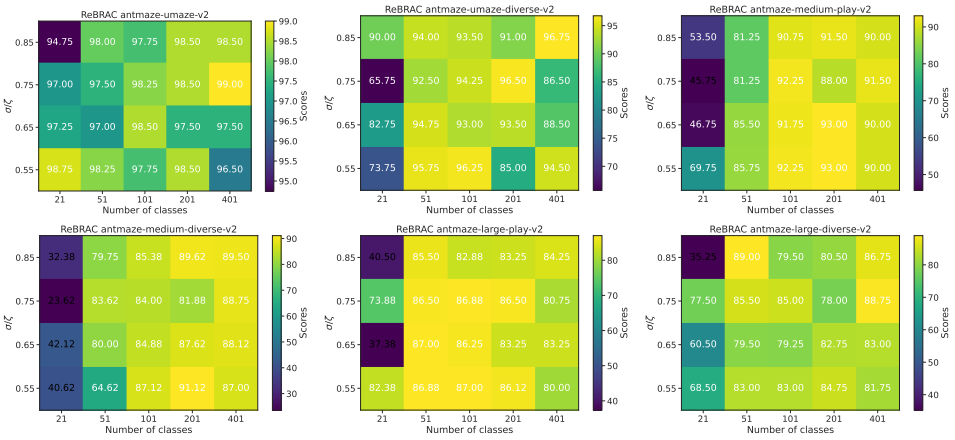

Figure 7: Heatmaps for the impact of the classification parameters on AntMaze datasets for ReBRAC.

I.3 ReBRAC, Adroit

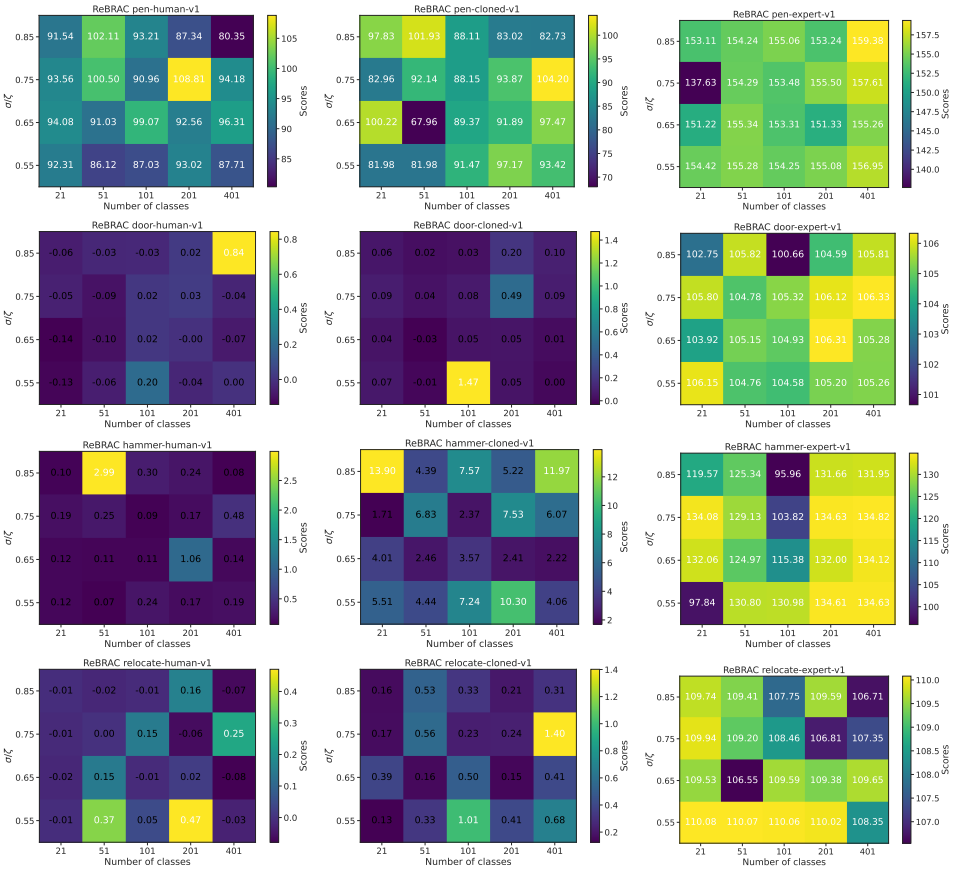

Figure 8: Heatmaps for the impact of the classification parameters on Adroit datasets for ReBRAC.

I.4 IQL, Gym-MuJoCo

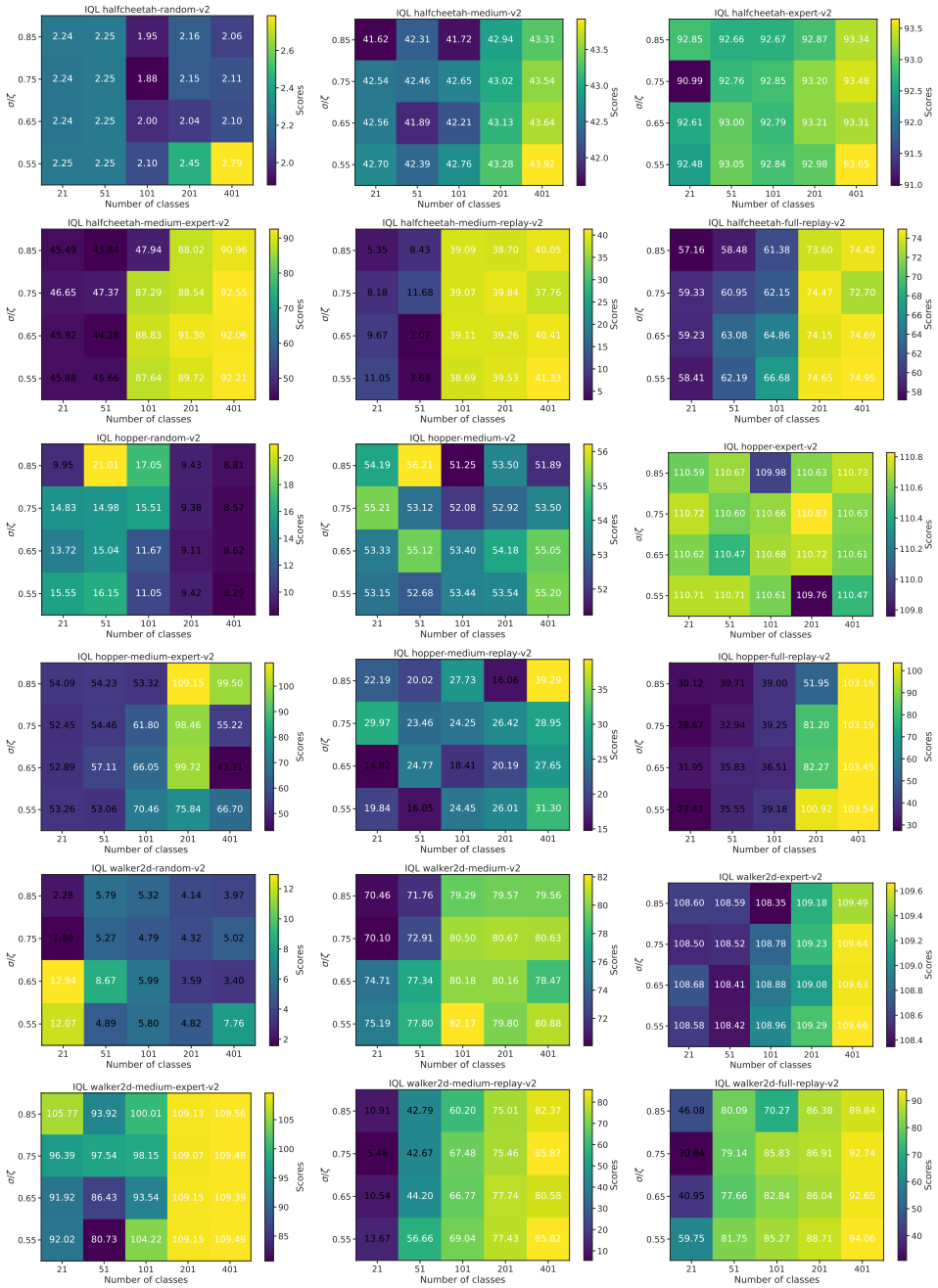

Figure 9: Heatmaps for the impact of the classification parameters on Gym-MuJoCo datasets for IQL.

I.5 IQL, AntMaze

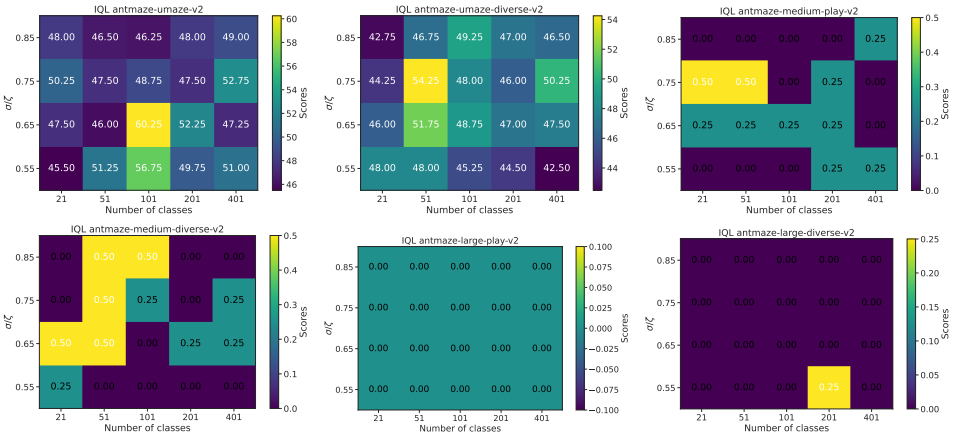

Figure 10: Heatmaps for the impact of the classification parameters on AntMaze datasets for IQL.

I.6 IQL, Adroit

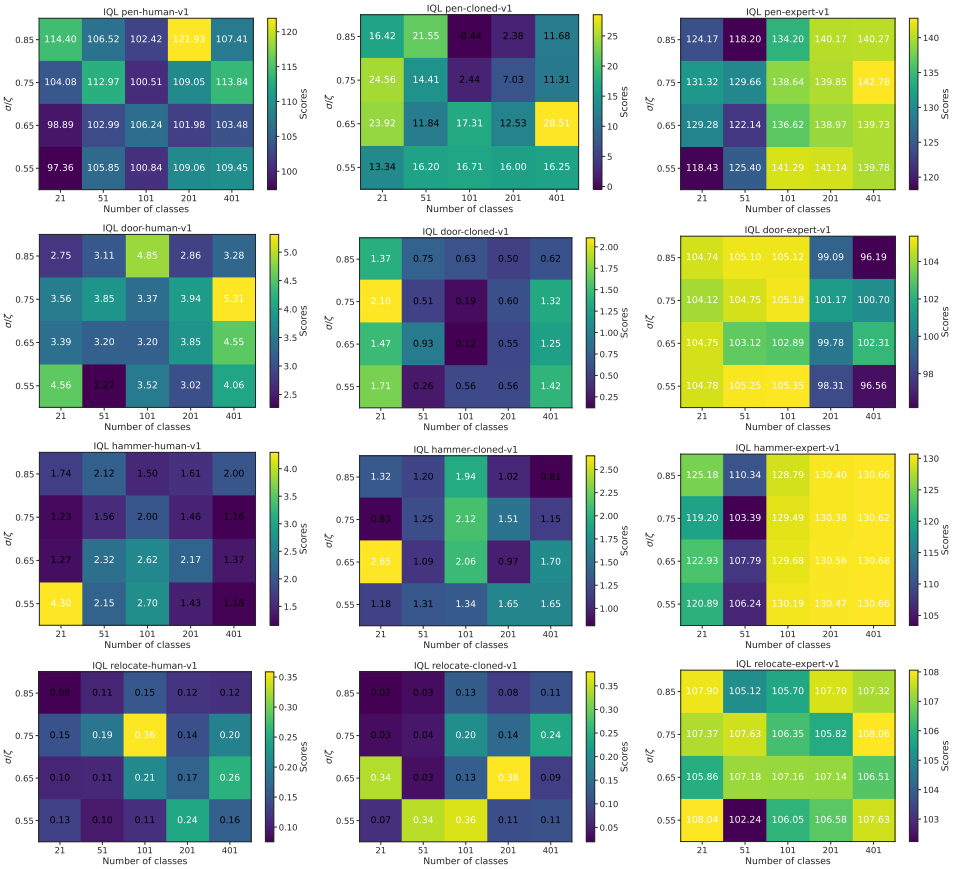

Figure 11: Heatmaps for the impact of the classification parameters on Adroit datasets for IQL.

I.7 LB-SAC, Gym-MuJoCo

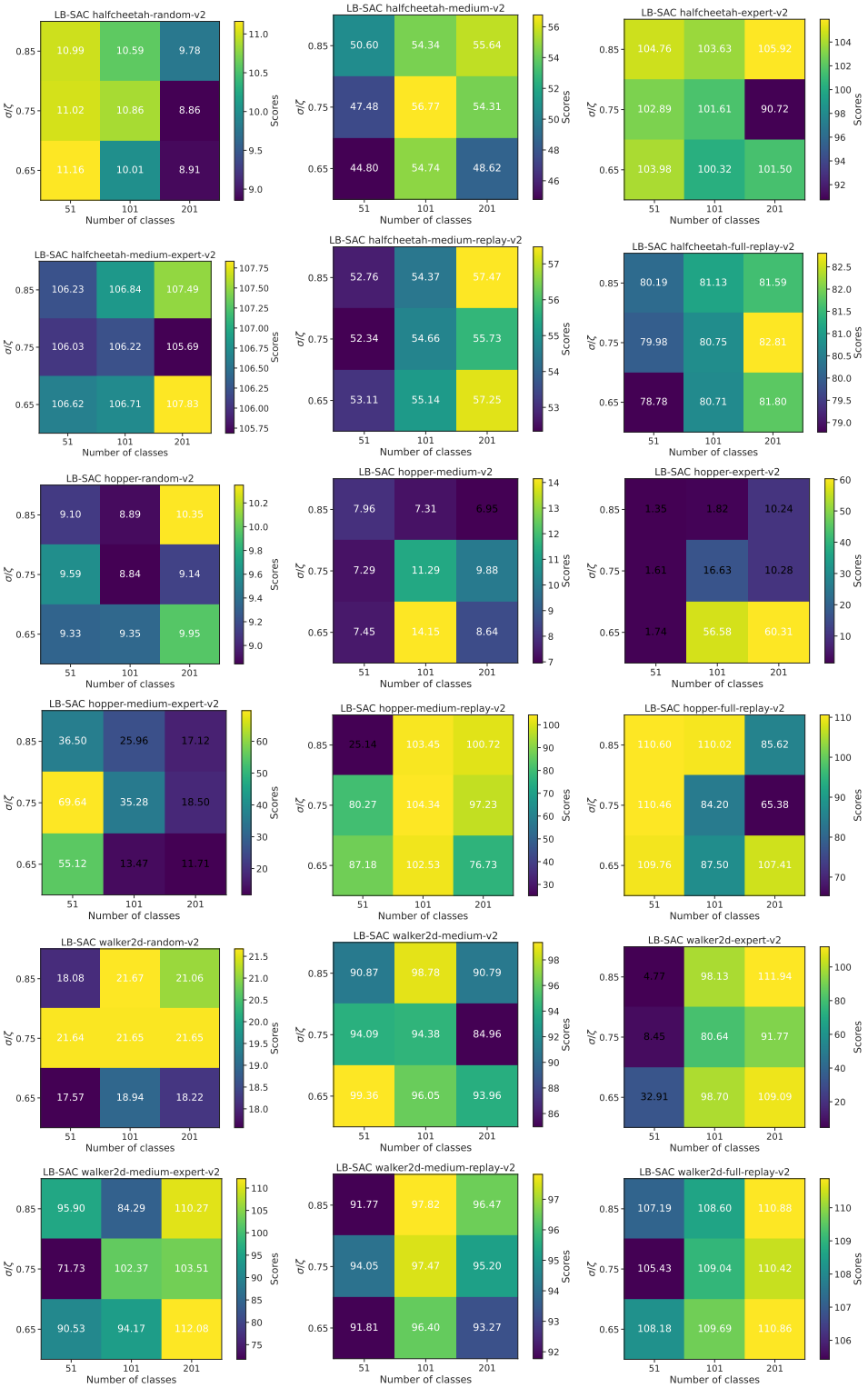

Figure 12: Heatmaps for the impact of the classification parameters on Gym-MuJoCo datasets for LB-SAC.

I.8 LB-SAC, AntMaze

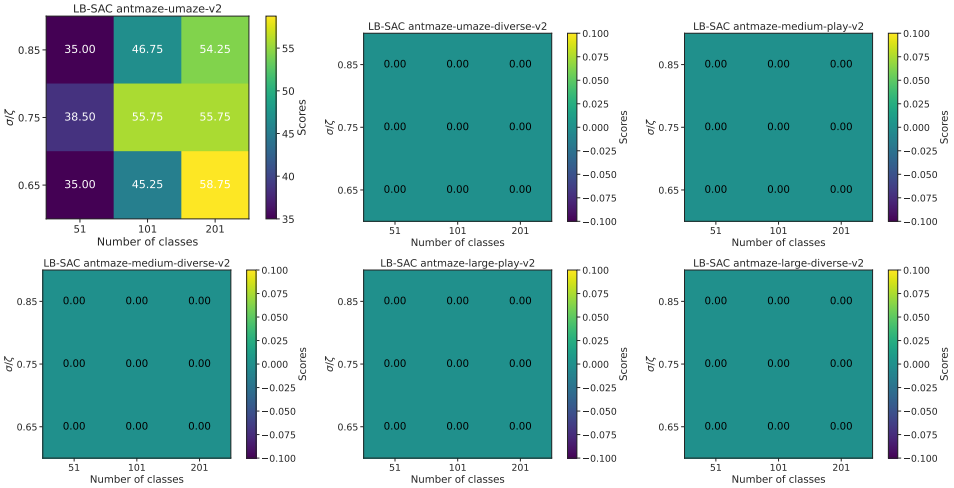

Figure 13: Heatmaps for the impact of the classification parameters on AntMaze datasets for LB-SAC.

I.9 LB-SAC, Adroit

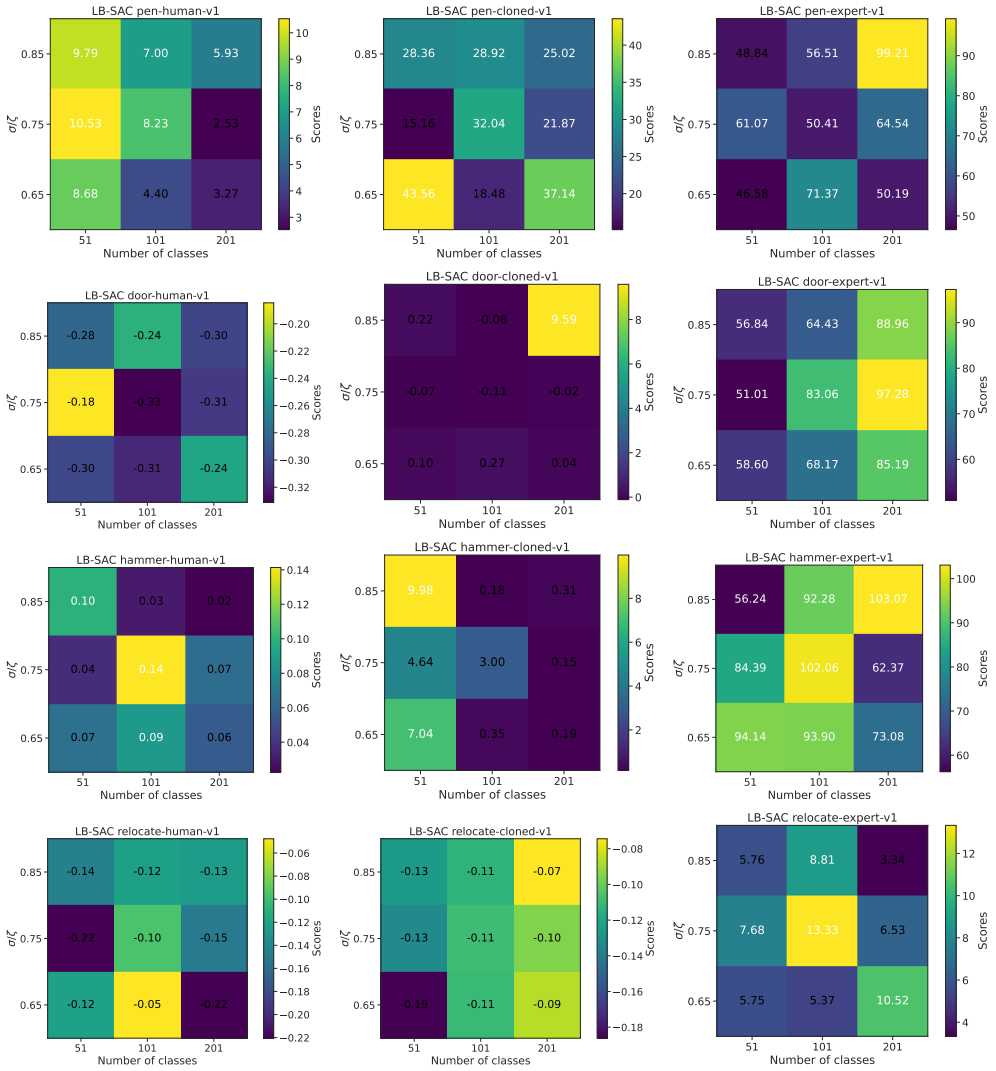

Figure 14: Heatmaps for the impact of the classification parameters on Adroit datasets for LB-SAC.